In HIV-1-infected brain, gp120, shed from virions and/or secreted from HIV-1-infected microglia/macrophages, has the potential to diffuse and interact directly with surrounding and distant neural cells through activation of CXCR4 receptors(Bachis and Mocchetti, 2004; Hesselgesser et al., 1998; Meucci et al., 1998), or by stimulation of uninfected microglia to release neurotoxins which act indirectly on local and distant neural cells, or both. Transgenic mice expressing gp120 manifest a spectrum of neuronal and glial changes resembling abnormalities in brains of HIV-1-infected humans and the severity of damage correlated positively with brain levels of gp120 expression (Toggas et al., 1994). While the precise mechanisms on how gp120 stimulates microglia production of neurotoxins remains to be determined, the enhancement of outward K^+ current by gp120 through CXCR4 may represent one of such potential mechanisms, as microglia-associated neurotoxicity was blocked either by a CXCR4 antagonist or by K_v channel blockers.

Microglia express a defined pattern of K_v channels, which is distinct from other glial cells and neurons. This pattern undergoes defined changes with microglia activation. It is believed that microglia K_v channels, albeit in a lower density than their excitable counterparts, play an important role in the switch from one functional state to another (Farber and Kettenmann, 2005; Kotecha and Schlichter, 1999). Patch clamp studies of microglia in cell cultures and in tissue slices have demonstrated that outward rectifier $K_v1.3$ and $K_v1.5$ are dominant K_v channels (Eder, 1998; Kotecha and Schlichter, 1999; Newell and Schlichter, 2005; Pannasch et al., 2006; Schilling et al., 2000). Our results showed that elevated levels of $K_v1.3$ expression and enhanced outward K^+ currents were detected in gp120-stimulated microglia and that the neuronal apoptosis induced by gp120-stimulated microglia was blocked by K_v channel blockers. These results suggest that gp120-induced elevation of K_v channel expression and enhancement of outward K^+ current might trigger microglia-associated neurotoxicity. Whereas the functional roles of $K_v1.3$ in microglia remain to be determined, evidence from this study and others indicates that the newly formed $K_v1.3$ channels appear to be involved in microglia activation and subsequent production of neurotoxins (Eder, 1998, 2005; Fordyce et al., 2005; Kotecha and Schlichter, 1999).

Ion channels are the targets of many intracellular signaling pathways including protein phosphorylation. These processes can modify channel activity and alter cellular electrophysiological properties. Thus, protein phosphorylation is an important physiological regulator of K_v channel function. Amino acid sequences of $K_v1.3$ clones from mouse, rats and human are very similar, with >98% homology between human and rat clones (Chandy and Gutman, 1995). All $K_v1.3$ clones contain several potential PKA and PKC phosphorylation sites, with one strong PKA site at the COOH terminus (Kennelly and Krebs, 1991). Evidence that $K_v1.3$ channels can be regulated by PKA includes reports of enhancement of delayed rectifier K^+ currents in vascular smooth muscle cells (Aiello et al., 1995), squid giant axon (Perozo et al., 1989) and human T lymphocytes (Chung and Schlichter, 1997). Inhibition of serine/threonine protein phosphatases with okadaic acid increases $K_v1.3$ current and shifts the voltage dependence of activation and inactivation to more positive potentials. Inhibition of PKA by a specific PKA inhibitor decreases $K_v1.3$ current. These observations indicate that $K_v1.3$ activity can be regulated by serine/threonine phosphorylation. The results obtained in this study revealed that the gp120-induced enhancement of microglia outward K^+ current was blocked by a specific PKA inhibitor H89, suggesting that activation of CXCR4 by gp120 in microglia causes cAMP-dependent PKA activation, resulting in $K_v1.3$ phosphorylation and consequent enhancement of channel activity.

$K_v1.3$ is predominantly expressed in immunocytes including microglia, lymphocytes, and macrophages and is important for immunocyte-mediated immune and inflammatory responses (Beeton et al., 2006; Chandy et al., 2004). Mounting evidence suggests that immune and inflammatory responses mediated by the activated microglia, the predominant resident CNS cell type productively infected by HIV-1(Lipton and Gendelman, 1995), play a pivotal role in the pathogenesis of HAND (Dheen et al., 2007; Garden, 2002; Glass and Wesselingh, 2001). Thus, studies on identification of specific target(s) to regulate microglia activation and resultant production of neurotoxins are highly imperative. Our results, gp120-associated neurotoxicity was blocked by a specific $K_v1.3$ blocker MgTx, indicate that $K_v1.3$ expressed in microglia may function as a potential target for the development of therapeutic strategies for HAND and perhaps for other neurodegenerative disorders. We anticipate that blockade of $K_v1.3$ channels in microglia might attenuate microglia-associated neurotoxicity, resulting in the protection of neurons from HIV-associated challenge in the infected brain. It is worth pointing out that there may be side effects by systemic or intracranial administration of $K_v1.3$ blockers since small amounts of $K_v1.3$ are also expressed in several brain regions such as hippocampus, and pyriform cortex (Kues and Wunder, 1992). However, such potential side effects might be minimal as animals deficient in $K_v1.3$ exhibited only a heightened sense of smell and distinct structure alterations in the olfactory bulb (Fadool et al., 2004). Thus, the potential for development of specific $K_v1.3$ blockers to suppress microglia-associated neurotoxicity is optimistic.

In summary, the experimental data provide *in vitro* evidence that HIV-1gp120 enhances outward K^+ current in cultured rat microglia via CXCR4 → cAMP-dependent PKA signaling pathway. Gp120 elevates the levels of K_v channel expression and alters K_v channel biophysical properties. Biological significance of gp120 enhancement of microglia outward K^+ current was demonstrated by experimental results that blockade of microglia K_v channels by K_v channel blockers suppresses microglia-induced neurotoxicity. As such, the K_v channel

expressed in microglia may function as a potential target in the development of therapeutic strategies for neurodegenerative disorders by which the activated resident microglia play a critical role in the pathogenesis.

ACKNOWLEDGMENTS

The authors thank Mr. Bryan Katafiasz for reading the manuscript. The authors extend special thanks to Ms. Julie Ditter, Ms. Robin Taylor, and Ms. Johna Belling for their excellent administrative supports and to two anonymous reviewers for their critical criticisms and helpful comments.

REFERENCES

Aiello EA, Walsh MP, Cole WC. 1995. Phosphorylation by protein kinase A enhances delayed rectifier K+ current in rabbit vascular smooth muscle cells. Am J Physiol 268:H926–H934.

Albright AV, Shieh JT, Itoh T, Lee B, Pleasure D, O'Connor MJ, Doms RW, Gonzalez-Scarano F. 1999. Microglia express CCR5, CXCR4, and CCR3, but of these, CCR5 is the principal coreceptor for human immunodeficiency virus type 1 dementia isolates. J Virol 73:205–213.

Bachis A, Mocchetti I. 2004. The chemokine receptor CXCR4 and not the N-methyl-D-aspartate receptor mediates gp120 neurotoxicity in cerebellar granule cells. J Neurosci Res 75:75–82.

Beeton C, Wulff H, Standifer NE, Azam P, Mullen KM, Pennington MW, Kolski-Andreaco A, Wei E, Grino A, Counts DR, others. 2006. Kv1.3 channels are a therapeutic target for T cell-mediated autoimmune diseases. Proc Natl Acad Sci U S A 103:17414–17419.

Chandy KG, Gutman GA. 1995. Voltage-gated potassium channel genes. In: North RA, editor. Ligand and Voltage-gated Ion Channels. Bpca Raton, FL: CRC. pp 1–71.

Chandy KG, Wulff H, Beeton C, Pennington M, Gutman GA, Cahalan MD. 2004. K+ channels as targets for specific immunomodulation. Trends Pharmacol Sci 25:280–289.

Chung I, Schlichter LC. 1997. Regulation of native Kv1.3 channels by cAMP-dependent protein phosphorylation. Am J Physiol 273:C622–C633.

Dheen ST, Kaur C, Ling EA. 2007. Microglial activation and its implications in the brain diseases. Curr Med Chem 14:1189–1197.

Eder C. 1998. Ion channels in microglia (brain macrophages). Am J Physiol 275:C327–C342.

Eder C. 2005. Regulation of microglial behavior by ion channel activity. J Neurosci Res 81:314–321.

Eder C, Fischer HG, Hadding U, Heinemann U. 1995. Properties of voltage-gated currents of microglia developed using macrophage colony-stimulating factor. Pflugers Arch 430:526–533.

Elkabes S, Peng L, Black IB. 1998. Lipopolysaccharide differentially regulates microglial trk receptor and neurotrophin expression. J Neurosci Res 54:117–122.

Fadool DA, Tucker K, Perkins R, Fasciani G, Thompson RN, Parsons AD, Overton JM, Koni PA, Flavell RA, Kaczmarek LK. 2004. Kv1.3 channel gene-targeted deletion produces "Super-Smeller Mice" with altered glomeruli, interacting scaffolding proteins, and biophysics. Neuron 41:389–404.

Fakler B, Brandle U, Glowatzki E, Zenner HP, Ruppersberg JP. 1994. Kir2.1 inward rectifier K+ channels are regulated independently by protein kinases and ATP hydrolysis. Neuron 13:1413–1420.

Farber K, Kettenmann H. 2005. Physiology of microglial cells. Brain Res Brain Res Rev 48:133–143.

Fischer HG, Eder C, Hadding U, Heinemann U. 1995. Cytokine-dependent K+ channel profile of microglia at immunologically defined functional states. Neuroscience 64:183–191.

Fordyce CB, Jagasia R, Zhu X, Schlichter LC. 2005. Microglia Kv1.3 channels contribute to their ability to kill neurons. J Neurosci 25: 7139–7149.

Garden GA. 2002. Microglia in human immunodeficiency virus-associated neurodegeneration. Glia 40:240–251.

Gendelman HE, Eiden L, Epstein L, Grant I, Lipton SA, McArthur JC, Pomerantz R, Price R, Swindells S. 1997. Neuropathogenesis of HIV-1 Dementia: A Panel Discussion. New York: Chapman & Hall.

Genis P, Jett M, Bernton EW, Boyle T, Gelbard HA, Dzenko K, Keane RW, Resnick L, Mizrachi Y, Volsky DJ, others. 1992. Cytokines and arachidonic metabolites produced during human immunodeficiency virus (HIV)-infected macrophage-astroglia interactions: implications for the neuropathogenesis of HIV disease. J Exp Med 176:1703–1718.

Glass JD, Wesselingh SL. 2001. Microglia in HIV-associated neurological diseases. Microsc Res Tech 54:95–105.

Hesselgesser J, Taub D, Baskar P, Greenberg M, Hoxie J, Kolson DL, Horuk R. 1998. Neuronal apoptosis induced by HIV-1 gp120 and the chemokine SDF-1 alpha is mediated by the chemokine receptor CXCR4. Curr Biol 8:595–598.

Kaul M, Garden GA, Lipton SA. 2001. Pathways to neuronal injury and apoptosis in HIV-associated dementia. Nature 410:988–994.

Kennelly PJ, Krebs EG. 1991. Consensus sequences as substrate specificity determinants for protein kinases and protein phosphatases. J Biol Chem 266:15555–15558.

Kielian T. 2004. Microglia and chemokines in infectious diseases of the nervous system: Views and reviews. Front Biosci 9:732–750.

Knaus HG, Koch RO, Eberhart A, Kaczorowski GJ, Garcia ML, Slaughter RS. 1995. [125I]margatoxin, an extraordinarily high affinity ligand for voltage-gated potassium channels in mammalian brain. Biochemistry 34:13627–13634.

Koenig S, Gendelman HE, Orenstein JM, Dal Canto MC, Pezeshkpour GH, Yungbluth M, Janotta F, Aksamit A, Martin MA, Fauci AS. 1986. Detection of AIDS virus in macrophages in brain tissue from AIDS patients with encephalopathy. Science 233:1089–1093.

Kotecha SA, Schlichter LC. 1999. A Kv1.5 to Kv1.3 switch in endogenous hippocampal microglia and a role in proliferation. J Neurosci 19:10680–10693.

Kues WA, Wunder F. 1992. Heterogeneous Expression Patterns of Mammalian Potassium Channel Genes in Developing and Adult Rat Brain. Eur J Neurosci 4:1296–1308.

Lavi E, Strizki JM, Ulrich AM, Zhang W, Fu L, Wang Q, O'Connor M, Hoxie JA, Gonzalez-Scarano F. 1997. CXCR-4 (Fusin), a co-receptor for the type 1 human immunodeficiency virus (HIV-1), is expressed in the human brain in a variety of cell types, including microglia and neurons. Am J Pathol 151:1035–1042.

Lipton SA, Gendelman HE. 1995. Seminars in medicine of the Beth Israel Hospital, Boston Dementia associated with the acquired immunodeficiency syndrome [see comments]. N Engl J Med 332:934–940.

Menteyne A, Levavasseur F, Audinat E, Avignone E. 2009. Predominant functional expression of Kv1.3 by activated microglia of the hippocampus after Status epilepticus. PLoS One 4:e6770

Meucci O, Fatatis A, Simen AA, Bushell TJ, Gray PW, Miller RJ. 1998. Chemokines regulate hippocampal neuronal signaling and gp120 neurotoxicity. Proc Natl Acad Sci U S A 95:14500–14505.

Miwa T, Furukawa S, Nakajima K, Furukawa Y, Kohsaka S. 1997. Lipopolysaccharide enhances synthesis of brain-derived neurotrophic factor in cultured rat microglia. J Neurosci Res 50:1023–1029.

Newell EW, Schlichter LC. 2005. Integration of K+ and Cl- currents regulate steady-state and dynamic membrane potentials in cultured rat microglia. J Physiol 567:869–890.

Norenberg W, Gebicke-Haerter PJ, Illes P. 1994. Voltage-dependent potassium channels in activated rat microglia. J Physiol 475:15–32.

Pannasch U, Farber K, Nolte C, Blonski M, Yan Chiu S, Messing A, Kettenmann H. 2006. The potassium channels Kv1.5 and Kv1.3 modulate distinct functions of microglia. Mol Cell Neurosci 33:401–411.

Perozo E, Bezanilla F, Dipolo R. 1989. Modulation of K channels in dialyzed squid axons. ATP-mediated phosphorylation. J Gen Physiol 93: 1195–1218.

Schilling T, Quandt FN, Cherny VV, Zhou W, Heinemann U, Decoursey TE, Eder C. 2000. Upregulation of Kv1.3 K(+) channels in microglia deactivated by TGF-beta. Am J Physiol Cell Physiol 279:C1123–C1134.

Toggas SM, Masliah E, Rockenstein EM, Rall GF, Abraham CR, Mucke L. 1994. Central nervous system damage produced by expression of the HIV-1 coat protein gp120 in transgenic mice. Nature 367:188–193.

Walz W, Bekar LK. 2001. Ion channels in cultured microglia. Microsc Res Tech 54:26–33.

Cellular & Molecular Immunology (2011) 8, 305–314

www.nature.com/cmi

RESEARCH ARTICLE

The increase in surface CXCR4 expression on lung extravascular neutrophils and its effects on neutrophils during endotoxin-induced lung injury

Mitsuhiro Yamada[1], Hiroshi Kubo[2], Seiichi Kobayashi[3], Kota Ishizawa[2], Mei He[2], Takaya Suzuki[2], Naoya Fujino[2], Hiroyuki Kunishima[1], Masamitsu Hatta[1], Katsushi Nishimaki[4], Tetsuji Aoyagi[4], Kouichi Tokuda[4], Miho Kitagawa[4], Hisakazu Yano[5], Hirokazu Tamamura[6], Nobutaka Fujii[7] and Mitsuo Kaku[1,4]

Inflammatory stimuli, such as a microbes or lipopolysaccharides, induce a rapid release of neutrophils from the bone marrow and promote neutrophil migration into inflamed sites to promote host defense. However, an excess accumulation and retention of neutrophils in inflamed tissue can cause severe tissue injuries in the later stages of inflammation. Recent studies have reported that both CXCL12 levels in injured lungs and its receptor, CXCR4, on accumulated neutrophils in injured lungs, increased; furthermore, these studies showed that the CXCL12/CXCR4 signaling pathway participated in neutrophil accumulation in the later stages of lipopolysaccharide (LPS)-induced lung injury. However, the mechanisms underlying this increase in surface CXCR4 expression in neutrophils remain unclear. In this study, we found that surface CXCR4 expression increased in extravascular, but not intravascular, neutrophils in the lungs of LPS-induced lung injury model mice. Furthermore, *ex vivo* studies revealed that CXCL12 acted not only as a chemoattractant, but also as a suppressor of cell death for the lung neutrophils expressing CXCR4. Sulfatide, one of the native ligands for L-selectin, induced the increase of surface CXCR4 expression on isolated circulating neutrophils, suggesting that the activation of L-selectin may be involved in the increase in surface CXCR4. Our findings show that surface CXCR4 levels on neutrophils increase after extravasation into injured lungs, possibly through the activation of L-selectin. The CXCL12/CXCR4 signaling pathway plays an important role in the modulation of neutrophil activity during acute lung injury, not only by promoting chemotaxis but also by suppressing cell death.
Cellular & Molecular Immunology (2011) **8,** 305–314; doi:10.1038/cmi.2011.8; published online 4 April 2011

Keywords: CXCL12; CXCR4; lipopolysaccharides; lung injury; neutrophils

INTRODUCTION

During acute inflammation, neutrophils are released from the bone marrow and migrate into inflamed tissues.[1,2] In inflamed tissues, neutrophils extravasate from blood vessels to the site of tissue injury or infection. These extravasated neutrophils play an important role in host defense against pathogenic microorganisms, though the excess accumulation and activation of neutrophils can cause severe tissue injury. Therefore, the apoptosis of neutrophils and the proper processing of apoptotic neutrophils by macrophage phagocytosis are important for the resolution of inflammation to prevent tissue injury. It is well established that inflammatory cytokines (including TNF-α[3] and IL-1[4]) and neutrophil attractant CXC chemokines[5–7] are critically involved in the accumulation of neutrophils within injured tissues during the acute phase of inflammation. However, the mechanisms of neutrophil retention and withdrawal during the later phase of inflammation are not well understood and are still being investigated.

The accumulated evidence published thus far suggests that CXC chemokine CXCL12/stromal cell-derived factor-1, which was first described as a strong chemotactic factor for lymphocytes,[8–11] contributes to the control of the neutrophil life cycle through the activation of CXCR4. It has been reported that the CXCL12/CXCR4 signaling system plays an important role in the regulation of neutrophil homeostasis, including both the release of neutrophils from bone marrow into blood[12–15] and the homing of the circulating neutrophils to the bone marrow.[14,16] In addition to the evidence supporting the role of

[1]Department of Regional Cooperation for Infectious Diseases, Tohoku University Graduate School of Medicine, Sendai, Miyagi, Japan; [2]Department of Advanced Preventive Medicine for Infectious Disease, Tohoku University Graduate School of Medicine, Sendai, Miyagi, Japan; [3]Department of Respiratory Medicine, Japanese Red-Cross Ishinomaki Hospital, Ishinomaki, Miyagi, Japan; [4]Department of Infection Control and Laboratory Diagnostics, Tohoku University Graduate School of Medicine, Sendai, Miyagi, Japan; [5]Department of Clinical Microbiology with Epidemiological Research & Management and Analysis of Infectious Diseases, Tohoku University Graduate School of Medicine, Sendai, Miyagi, Japan; [6]Institute of Biomaterials and Bioengineering, Tokyo Medical and Dental University, Chiyoda-ku, Tokyo, Japan and [7]Graduate School of Pharmaceutical Sciences, Kyoto University, Kyoto, Japan
Correspondence: Dr H Kubo, Department of Advanced Preventive Medicine for Infectious Disease, Tohoku University Graduate School of Medicine, 2-1 Seiryoumachi, Aobaku, Sendai 980-8575, Japan.
E-mail: hkubo@med.tohoku.ac.jp
Received 9 December 2010; revised 8 February 2011; accepted 23 February 2011

CXCL12/CXCR4 in modulating neutrophil homeostasis, we and other investigators previously reported that both CXCL12 levels in the injured lungs and surface CXCR4 protein on accumulated neutrophils were increased; furthermore, the *in vivo* administration of an anti-CXCL12 blocking antibody suppressed airspace neutrophilia in the lungs in the later stages of lipopolysaccharide (LPS)-induced lung injury.[17–19] These findings suggested that this chemokine participated in the accumulation of neutrophils in the injured tissue, particularly in the later stages of inflammation. However, the mechanisms underlying the increase in surface CXCR4 expression on neutrophils during LPS-induced lung injury and the CXCL12-promoted accumulation of neutrophils remain unclear.

In this study, we investigated when and how surface CXCR4 expression levels increased on neutrophils in the lungs during LPS-induced lung injury. We further examined the effects of CXCL12 on isolated neutrophils to evaluate how this chemokine contributes to neutrophil accumulation in the injured tissue. In our investigation of the mechanism underlying the increase in surface CXCR4 expression levels, we focused on L-selectin because previous reports have shown that the activation of L-selectin induced the expression of surface CXCR4 in both human and mouse lymphocytes;[20,21] furthermore, the shedding of L-selectin, which resulted from the activation of L-selectin by its ligands,[22] was observed in extravasated neutrophils in inflamed tissues of mice.[23,24]

MATERIALS AND METHODS

Animals

C57BL/6J mice were purchased from CLEA Japan Inc. (Tokyo, Japan). All mice were 7- to 8-week-old males and were housed under specific pathogen-free conditions for 1 week prior to experimental use. All animal experiments were permitted by the Institutional Animal Care and Use Committee of the Tohoku University Environmental and Safety Committee and were performed in accordance with the Regulations for Animal Experiments and Related Activities at Tohoku University.

Reagents

The reagents used in this study were obtained from the following sources: mouse monoclonal anti-CXCL12 blocking antibody was purchased from R&D Systems (Minneapolis, MN, USA); control mouse immunoglobulin G1 (IgG1) was purchased from Sigma (St Louis, MO, USA); a specific CXCR4 antagonist, 4F-benzoyl-TE14011, was synthesized as previously described;[25,26] a rabbit anti-mouse CXCL12 antibody was purchased from BioVision (Mountain View, CA, USA) for immunohistochemical experiments; mouse monoclonal anti-mouse/human CXCL12 antibody was purchased from R&D Systems for immunoblotting analysis; phycoerythrin (PE)-conjugated rat anti-mouse CXCR4 monoclonal antibody (clone 2B11/CXCR4) and an isotype control antibody (clone A95-1), PE-conjugated rat IgG2b), fluorescein isothiocyanate (FITC)-conjugated rat anti-mouse Ly-6G monoclonal antibody (clone 1A8) and purified rat anti-mouse CD16/CD32 (Fcγ III/II receptor) monoclonal antibody (clone 2.4G2, Mouse BD Fc Block) were purchased from BD Pharmingen (San Diego, CA, USA); FITC-conjugated anti-mouse neutrophil antibody (clone 7/4) was purchased from Serotec (Raleigh, NC, USA); Alexa Fluor 647-conjugated anti-mouse Ly-6G (Gr-1) monoclonal antibody (clone RB6-8C5), 7-aminoactinomycin D (7-AAD) viability staining solution and an Annexin V apoptosis detection kit APC were purchased from eBioscience (San Diego, CA, USA); Alexa Fluor 647 anti-mouse CD62L antibody and Alexa Fluor 647 rat IgG2a, κ isotype control antibody were purchased from Biolegend (San Diego, CA, USA); recombinant mouse CXCL12α was purchased from R&D Systems; sulfatide sodium salt from bovine spinal cord was purchased from Wako Chemicals (Tokyo, Japan); TRIzol reagent was purchased from Invitrogen (Carlsbad, CA, USA); anti-p44/42 MAPK (ERK1/2) rabbit monoclonal antibody, anti-phospho-p44/42 MAPK (ERK1/2, Thr202 and Tyr204) rabbit monoclonal antibody, anti-Akt rabbit monoclonal antibody, anti-phospho-Akt (Thr308) rabbit monoclonal antibody, goat anti-rabbit IgG, HRP-linked antibody, cell lysis buffer, U0126 (MEK1/2 inhibitor) and LY294002 (PI3 kinase inhibitor) were purchased from Cell Signaling Technology (Danvers, MA, USA).

LPS-induced lung injury

LPS from *Escherichia coli* serotype 055:B5 was obtained from Sigma. Mice were anesthetized by ketamine hydrochloride. While anesthetized, mice intranasally inhaled LPS (20 μg/mouse in phosphate-buffered saline (PBS)) that was placed on one nostril. Control mice received only PBS.

Preparation of single lung cells from lungs

Mice received an overdose of inhaled halothane, and their lungs were perfused with PBS *via* the right ventricles. PBS-perfused lungs were isolated with other mediastinal organs. Dispase II solution was instilled into the lungs through the trachea, which was ligated with a silk suture. After incubation at 37 °C for 50 min, the lungs were separated from the other mediastinal organs. The lungs were then thoroughly minced and digested in PBS with 0.1% collagenase, 0.01% deoxyribonuclease I and 5-mM $CaCl_2$ at 37 °C for 20 min. The cells were then suspended in red blood cell lysing buffer to remove red blood cells and subsequently washed with PBS. The cells were then centrifuged and resuspended in PBS.

Evaluation of surface CXCR4 expression on neutrophils

The surface CXCR4 expression levels of neutrophils isolated from bone marrow, circulating blood, single lung cell suspensions and BAL fluid were evaluated. Mouse neutrophils were identified by their forward scatter and side scatter characteristics and positive Ly-6G staining. The samples were stained with a PE-labeled anti-CXCR4 antibody or a PE-labeled isotype-matched control antibody and an FITC-labeled anti-Ly6G (1A8) antibody. Dead cells were excluded based on 7-AAD staining. The samples were analyzed using a FACSCalibur flow cytometer (BD Biosciences, San Jose, CA, USA).

Identification of intravascular and extravascular neutrophils in the lungs

The identification of intravascular and extravascular neutrophils in the lungs was performed as previously described with some modifications.[27] An Alexa Fluor 647-conjugated anti-mouse Ly-6G (Gr-1) antibody (1 μg) was injected intravenously and allowed to circulate for 5 min. After 5 min, the mice were killed. The lungs were then digested as described above in the presence of an excess of unlabeled anti-mouse Gr-1 antibody to prevent possible binding of Alexa Fluor 647-conjugated anti-Gr-1 antibody to extravascular neutrophils. The lung cell suspensions were then stained with an FITC-conjugated anti-mouse neutrophil antibody (7/4). Intravascular ($7/4^+Gr\text{-}1^+$) and extravascular ($7/4^+Gr\text{-}1^-$) neutrophil populations were assessed using flow cytometry.

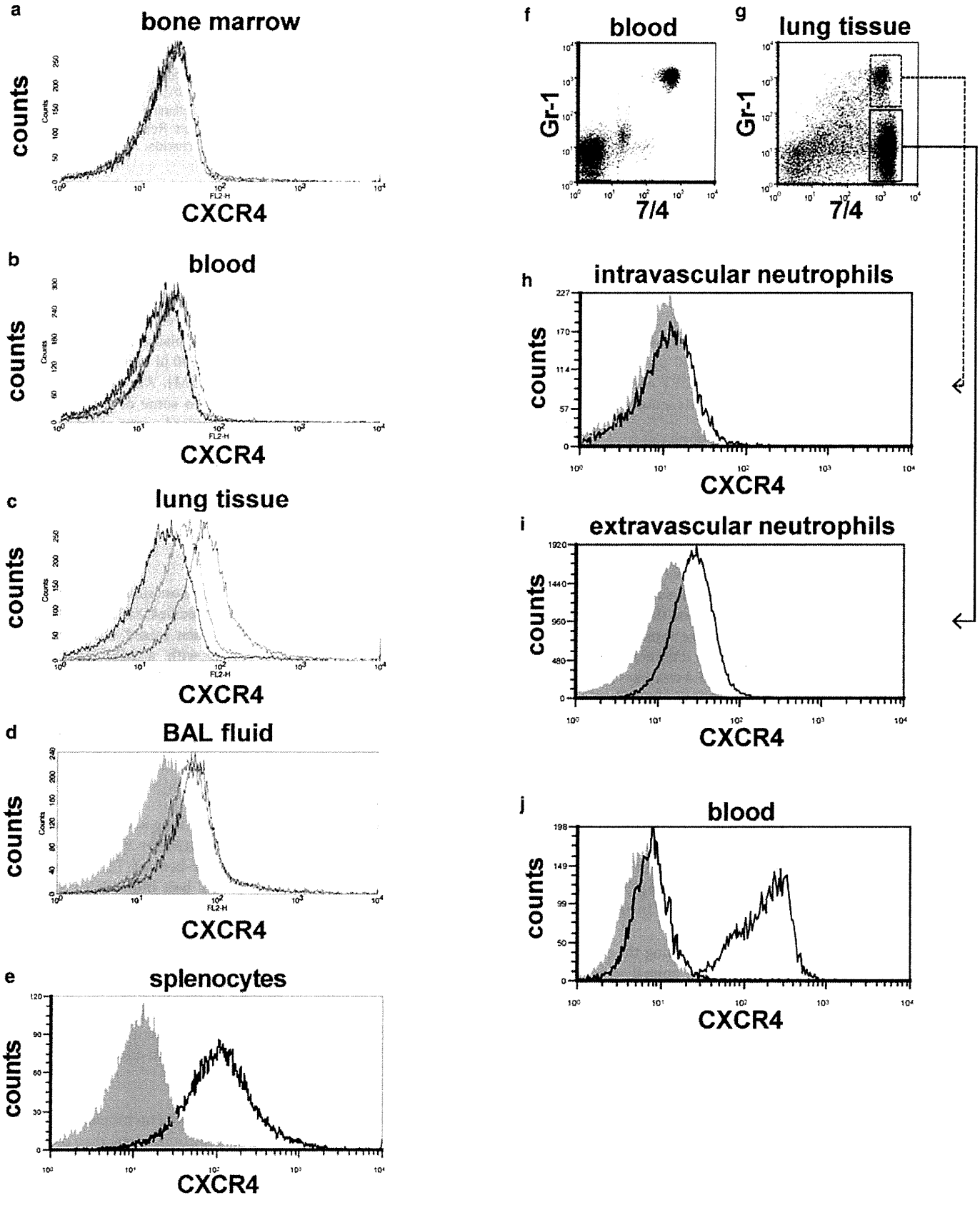

Figure 1 Surface CXCR4 expression increased in extravascular neutrophils in the mouse lungs during LPS-induced lung injury. (**a**–**e**) Flow cytometric analyses were performed to determine the surface CXCR4 expression levels of neutrophils isolated from bone marrow (**a**), peripheral blood (**b**), lung tissue (**c**) and BAL fluid (**d**). Neutrophils were analyzed before LPS administration (black line) and at 6 h (red line) and 24 h (blue line) afterward. The filled images show the staining using an

isotype-matched control antibody. We were unable to analyze the surface CXCR4 expression levels of neutrophils isolated from BAL fluid before LPS administration because there were an insufficient number of neutrophils in these samples. Splenocytes from untreated control mice were used as a positive control for CXCR4 staining (**e**). (**f–i**) The surface CXCR4 expression levels of intravascular neutrophils (**g**; GR-1$^+$7/4$^+$) and extravascular neutrophils (**g**; GR-1$^-$7/4$^+$) in the lungs at 24 h during LPS-induced lung injury were examined. Note almost all circulating neutrophils (7/4$^+$ cells) in blood were stained with Gr-1 5 min after antibody injection (**f**). The blue lines show the surface CXCR4 expression levels of intravascular neutrophils (**h**) or extravascular neutrophils (**i**). The filled images show the staining using an isotype-matched control antibody. (**h**) The levels of intracellular CXCR4 (blue line) in neutrophils isolated from mouse blood were analyzed by staining with permeabilization. The filled image shows the staining using an isotype-matched control antibody. The black line shows the surface CXCR4 expression levels. Representative histograms or dot plots from one of three experiments that showed similar results are presented. BAL, bronchoalveolar lavage; LPS, lipopolysaccharide.

In vivo blocking the CXCL12/CXCR4 signaling pathway using a specific CXCR4 antagonist

A specific CXCR4 antagonist (4F-benzoyl-TE14011) was used for *in vivo* inhibition of the CXCL12/CXCR4 signaling pathway as described previously.[28] Briefly, 4F-benzoyl-TE14011 was dissolved in PBS and subcutaneously administered using ALZET osmotic pumps (Durect Corp., Cupertino, CA, USA) that were implanted dorsally under the skin 1 day before administration of LPS. 4F-benzoyl-TE14011 was infused at a rate of 120 μg/day for 3 days after implantation. For the control study, ALZET osmotic pumps filled with the same volume of PBS were subcutaneously implanted in the same manner.

Bronchoalveolar lavage (BAL)

First, mice were killed by administering an overdose of halothane. Lavage tubes were then implanted into the mice according to the following procedure: a median sternotomy was performed, the trachea were dissected and isolated from the underlying soft tissues and a 0.8-mm lavage tube was inserted through a small incision in the trachea. BAL was performed by instilling 0.5 ml of ice cold PBS into the lungs and then gently aspirating the fluid. BAL was then repeated two times using fresh 0.5-ml aliquots of PBS. These three fluid samples were pooled and centrifuged. Cell counts and differentials were then performed. BAL protein in cell-free BAL fluid was assayed as an index of lung injury and capillary leakage. Protein quantification was performed using a BCA Protein Assay Reagent Kit (Pierce Biotechnology Inc., Rockford, IL, USA).

Histological analysis

The lungs were fixed by inflation with 10% neutral-buffered formalin at a transpulmonary pressure of 20 cm H_2O, embedded in paraffin and cut into 5-μm thick sections. Sections were stained with hematoxylin and eosin for histological assessment. Images were taken with Nikon Eclipse E80i Microscope (Nikon, Tokyo, Japan). These images were analyzed using ImageJ software (National Institutes of Health, Bethesda, MD, USA).

The lung injury scores were calculated using the previously published scoring system.[29] Two sections per animal were scored independently. Alveolar wall thickness was quantified in a blinded fashion by measuring of all septa along a crosshair placed on each image. At least 200 septa per animal were measured. The number of emigrated neutrophils was quantified by counting the number neutrophils present within all alveolar spaces in randomly selected fields. At least 200 alveolar spaces were counted.

Isolation of lung neutrophils

Neutrophils were separated from bone marrow cells, circulating blood leukocytes and single lung cell suspensions using an anti-Ly6G (1A8) MicroBead Kit (Miltenyi Biotec, Bergisch Gladbach, Germany) according to the manufacturer's protocol. The purity of the isolated neutrophils was evaluated using both microscopic and flow cytometric analyses and was determined to be greater than 98%.

Neutrophil migration assay

Neutrophils were placed on a modified Boyden chamber with 3-μm pores (Chemotaxcell; Kurabo Industries Ltd, Osaka, Japan) to evaluate the migration stimulating activity of CXCL12. Splenocytes, which can migrate toward CXCL12,[26] were used as a positive control. A total of 5×10^5 neutrophils or splenocytes in 200 μl of RPMI 1640 medium containing 0.25% bovine serum albumin were placed in the upper chambers. The upper chambers were then placed in individual wells of a 24-well cell culture plate containing 500 μl of assay buffer either with or without mouse CXCL12α (50 nM). An equal number of neutrophils or splenocytes were added to some of the lower wells without a top chamber to provide a standard count of total cells. In some experiments, the cells were pre-incubated with 100-nM 4F-benzoyl-TE14011 at 37 °C for 30 min. The chambers were then incubated for 2 h at 37 °C. The cells in the lower chamber were collected, and the percentage of migration was determined from the original cell input.

Cell death analysis

Lung neutrophils (2×10^6) in RPMI 1640 containing 10% FCS were either untreated or preincubated with a specific CXCR4 antagonist for 1 h at 37 °C. The neutrophils were then mixed with 100 ng/ml CXCL12α alone or in combination with a MEK1/2 inhibitor (U0126, 1 μM) or a PI3K inhibitor (LY294002, 10 μM) and incubated for an additional 24 h at 37 °C. After this incubation, the neutrophils were counted and the percentage of dead cells was calculated using trypan blue staining. Neutrophils were also stained with Annexin V and 7-AAD, and then analyzed using a FACSCalibur flow cytometer.

Western blotting

Lung neutrophils isolated from the injured lung were left untreated or incubated at 37 °C with 100 ng/ml CXCL12α for 30 s. Some neutrophils were pre-incubated with 100-nM 4F-benzoyl-TE14011 at 37 °C for 30 min. Cells were lysed in 1× cell lysis buffer (Cell Signaling Technology). Whole-cell lysate was run on an any kD Mini-PROTEAN TGX Precast SDS-PAGE gel (Bio-Rad, Hercules, CA, USA) and the proteins were transferred by electroblotting onto polyvinylidene fluoride membrane (Invitrogen). The blots were probed with antibodies specific for ERK1/2 phosphorylation at Thr202 and Tyr204 or Akt phosphorylation at Thr 308. Membranes were stripped with Restore Western Blot Stripping Buffer (Thermo Fisher Scientific, Rockford, IL, USA) and then reblotted with anti-ERK1/2 or anti-Akt.

L-selectin stimulation

Neutrophils were resuspended in RPMI 1640 (Invitrogen) with 0.1% bovine serum albumin (Sigma). The neutrophils were then incubated with sulfatide at a final concentration of 100 μg/ml for 1 h at 37 °C.

Data presentation and statistical analysis

Unless otherwise noted, all data presented are expressed as mean± standard error of the mean (s.e.m.). Statistical analyses were performed using Statistica software (StatSoft Inc., Tulsa, OK, USA).

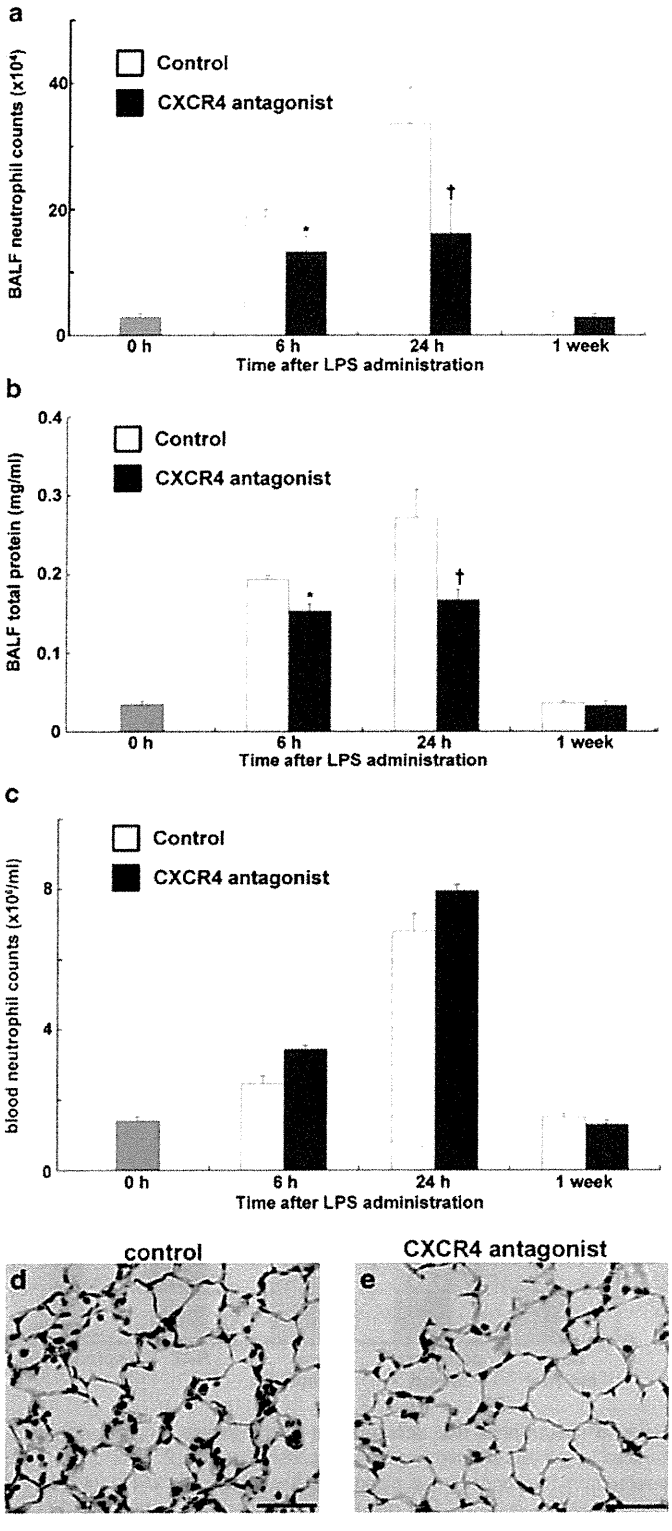

Figure 2 Blocking the CXCL12/CXCR4 signaling pathway inhibited neutrophil migration into the lung air space and the increase of lung permeability during LPS-induced lung injury. (**a–c**) Neutrophil counts (**a**), total protein concentration (**b**) in the BALF and neutrophil counts in the circulating blood (**c**) were determined in C57BL/6 mice treated with either PBS (white) or a CXCR4 antagonist (black) at indicated time points during LPS-induced lung injury. A total of six mice were used in each group. Values represent mean±s.e.m. **P*<0.01, †*P*<0.05, versus PBS control mice using ANOVA with Scheffé's *post hoc* test. (**d**, **e**) Histological evaluation of the treatment with a CXCR4 antagonist on LPS-induced lung injury. Representative images of hematoxylin and eosin stained lung tissue sections from PBS- (**d**) or CXCR4 antagonist-treated (**e**) mice at 24 h during LPS-induced lung injury. Scale bar=50 μm. BALF, bronchoalveolar lavage fluid; LPS, lipopolysaccharide; PBS, phosphate-buffered saline.

Data were assessed for significance by ANOVA with Scheffé's *post hoc* method for multiple comparisons. Statistical significance was defined as $P<0.05$.

RESULTS

The expression of surface CXCR4 increased on extravascular neutrophils in the mouse lungs during LPS-induced lung injury

Neutrophils in bone marrow, peripheral blood and lung digests from untreated control mice expressed very low levels of surface CXCR4 (Figure 1a–c, black lines). Surface expression of CXCR4 did not clearly increased in neutrophils from the bone marrow or peripheral blood at 6 and 24 h after LPS instillation (Figure 1a and b, red and blue lines, respectively). However, neutrophils from lung digests and BAL fluids exhibited a significant increase in surface CXCR4 expression at both 6 and 24 h during LPS-induced lung injury (Figure 1c and d, red and blue lines, respectively). To investigate whether a subset of neutrophils with higher surface CXCR4 expression in the blood emigrates into the lungs or if neutrophil surface CXCR4 expression increases after the cells emigrate into the lungs, we examined the surface CXCR4 expression of both intravascular and extravascular neutrophils in the lungs during LPS-induced lung injury. We first labeled intravascular neutrophils *in vivo* by the intravascular administration of the Alexa 647-conjugated anti-mouse Gr-1 antibody and labeled all neutrophils in the lung digest using the FITC-conjugated anti-mouse 7/4 antibody (Figure 1f and g, also see the section on 'Materials and methods'). Almost all circulating neutrophils in blood were stained with Gr-1 5 min after antibody injection (Figure 1f). Extravascular neutrophils, which were labeled with the anti-7/4 but not the anti-Gr-1 antibody (Figure 1g), exhibited clearly higher surface CXCR4 expression levels (Figure 1i) compared to intravascular neutrophils (Figure 1h). As previously reported in humans,[16] intracellular staining revealed that the levels of CXCR4 expression were high in the intracellular compartments of neutrophils isolated from mouse blood (Figure 1j), suggesting that translocation of CXCR4 to the cell surface occurred in the neutrophils isolated from injured lungs. Taken together, these findings suggested that the cell surface CXCR4 expression levels increased after these cells emigrated into the lungs and extravasated during LPS-induced lung injury.

Blocking the CXCL12/CXCR4 signaling pathway inhibited neutrophil accumulation into the air space and attenuated the increase in lung permeability during LPS-induced lung injury.

Previous reports by our group and other investigators have shown that CXCL12 levels are upregulated in injured lungs and that *in vivo* administration of anti-CXCL12 blocking antibodies suppresses airspace neutrophilia in the lungs at the later stages of LPS-induced lung injury,[17–19] suggesting that the increase of surface CXCR4 expression on lung extravasated neutrophils cooperates with the increase of CXCL12 in the lungs to facilitate the accumulation of neutrophils. To confirm the *in vivo* role of the CXCL12/CXCR4 signaling system in the pathogenesis of acute lung injury, we administrated a specific CXCR4 antagonist to block the activation of CXCR4. Because it has been reported that single-dose administration of a CXCR4 antagonist rapidly induces neutrophilia,[12,30,31] we administrated the antagonist continuously using an osmotic pump as previously we did.[28] We compared white blood cell and neutrophil count between

Table 1 Histopathological lung injury score, interalveolar septal thickness and the number of neutrophils in alveolar spaces in mice at 24 h during LPS-induced lung injury

Measure	*Untreated control*	*LPS and PBS*	*LPS and CXCR4 antagonist*
Lung injury score	1.1±0.1	3.3±0.1	2.5±0.2*
Septal thickness (μm)	1.6±0.1	2.9±0.1	2.5±0.1*
No. of neutrophils in 100 alveoli	1.2±0.3	68.3±4.6	48.5±2.9*

Abbreviations: LPS, lipopolysaccharide; PBS, phosphate-buffered saline.
Data are represented as mean±s.e.m. $n=6$ per group.
*$P<0.01$ versus LPS and PBS group.

subcutaneous single-dose and continuous dosing administration of 4F-benzoyl-TE14011 in uninjured mice. As previously reported in human,[30,31] single-dose administration of 4F-benzoyl-TE14011 caused the significant neutrophilia with a peak increase at 6 h (Supplementary Table 1). However, continuous dosing administration did not cause the significant neutrophilia (Supplementary Table 1). Continuous administration of the antagonist also did not result in significant neutrophilia in comparison with control mice during LPS-induced lung injury (Figure 2c). The number of the neutrophils (Figure 2a) and the protein concentration (Figure 2b) in the BAL fluid were significantly reduced in CXCR4 antagonist treated mice at 6 and 24 h during LPS-induced lung injury in comparison with the control mice. Histological assessment also revealed that the treatment with a CXCR4 antagonist attenuated the lung injury induced by LPS at 24 h (Figure 2e and c and Table 1). These findings confirmed that both CXCL12 and its receptor CXCR4 contribute to neutrophil accumulation in the air space and an increase in lung permeability during LPS-induced lung injury.

Neutrophils isolated from injured lungs exhibited migratory activity toward CXCL12

To elucidate the role of CXCR4 in the accumulation of neutrophils in the injured lung, we examined whether lung neutrophils responded to and showed the migratory activity toward CXCL12. Isolated neutrophils from the LPS-instilled mice were placed in modified Boyden chambers, and CXCL12 was added to the chambers as a chemoattractant. Splenocytes from untreated control mice were used as a positive control because splenocytes expressed high levels of surface CXCR4 (Figure 1e). Neutrophils isolated from the bone marrow or peripheral blood exhibited no migratory response toward CXCL12 (Figure 3). In contrast, neutrophils isolated from lung digests and BAL fluids exhibited migratory responses to CXCL12 (Figure 3). Furthermore, this migratory response to CXCL12 was blocked by a specific CXCR4 antagonist. These *ex vivo* findings demonstrated that the accumulated lung neutrophils expressing high surface levels of CXCR4 exhibited migratory activity toward CXCL12, whereas bone marrow and peripheral blood neutrophils, which express very low surface levels of CXCR4, did not respond to CXCL12.

Activation of CXCR4 by CXCL12 attenuated cell death of isolated neutrophils from the injured lungs

The observation that blocking the CXCL12/CXCR4 pathway decreased the number of neutrophils in the air space suggests the involvement in neutrophil recruitment during LPS-induced lung injury. However, in contrast to the enhanced migratory activity toward CXCL12 observed in the accumulated lung neutrophils, the blood neutrophils, which expressed very low levels of CXCR4 (Figure 1), did not exhibit a migratory response to CXCL12 (Figure 3). This suggested that the CXCL12/CXCR4 pathway was not critically involved in the recruitment of neutrophils, at least from circulating blood into the injured lungs. It has been reported that CXCR4 activation by CXCL12 suppressed cell death of $CD34^+$ hematopoietic cells[32] and $CD4^+$ T cells.[33] To investigate whether the CXCL12/CXCR4 pathway contributes to the accumulation of neutrophils in the injured lung by suppressing the neutrophil death, we examined the role of CXCL12 in suppressing cell death of the lung neutrophils. We performed trypan blue staining to assess cell death after *ex vivo* culture either with or without CXCL12. The administration of CXCL12 decreased cell death levels of the neutrophils (Figure 4a). This protective effect of CXCL12 against cell death was blocked by the administration of a specific CXCR4 antagonist (Figure 4b–d). We further performed Annexin V and 7-AAD staining to assess apoptosis levels after culture. The incidences of both early apoptotic cells and late apoptotic/necrotic cells were reduced by CXCL12. This protective effect against apoptosis was also blocked by a CXCR4 antagonist (Figure 4b–d).

We then investigated the mechanisms for how CXCL12/CXCR4 signaling protects neutrophils from apoptosis. We focused on both ERK and PI3K/Akt signaling pathways because it has been reported that CXCL12/CXCR4 signaling protects T cells,[33] $CD34^+$

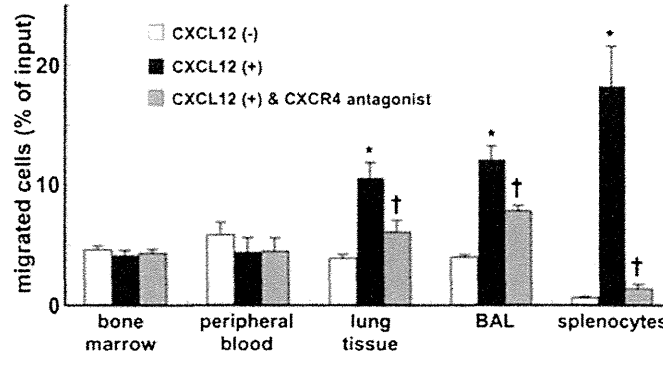

Figure 3 Neutrophils that accumulated in the mouse lungs during LPS-induced lung injury showed migratory responses to CXCL12. Neutrophils were isolated from the bone marrow, blood, lung tissue and BAL fluid at 24 h during LPS-induced lung injury. Cell migration assays assessing the migration of neutrophils toward CXCL12 were performed *in vitro* using chemotaxis chambers. Splenocytes from untreated control mice were used as a positive control because splenocytes expressed high levels of surface CXCR4 (Figure 1e). Levels of neutrophil or splenocyte migration in the absence of CXCL12, the presence of CXCL12, or after pretreatment with a CXCR4 antagonist in the presence of CXCL12, are depicted by the white, black and gray bars, respectively. The data shown represent the percentage of migration. The results were obtained from five mice in each group. Values represent mean±s.e.m. *$P<0.01$ versus CXCL12 (−) control group and †$P<0.01$ versus CXCL12 (+) group using ANOVA with Scheffé's *post hoc* test. BAL, bronchoalveolar lavage.

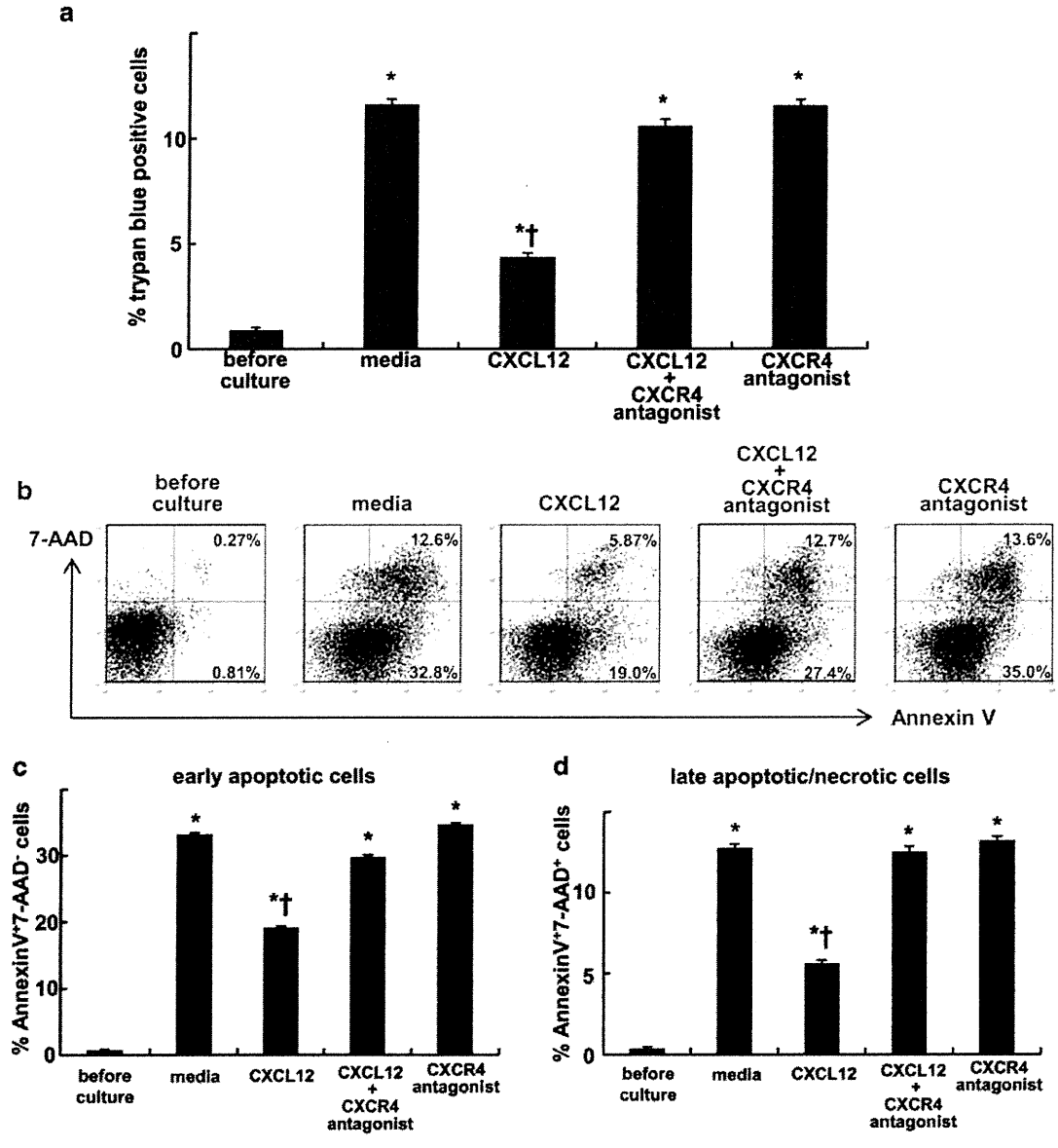

Figure 4 CXCR4 activation by CXCL12 attenuated the cell death of mouse neutrophils isolated from the injured lungs. Neutrophils were isolated from the mouse lungs at 24 h after LPS instillation. The isolated neutrophils were cultured in either media alone (RPMI 1640 supplemented with 10% FCS), media containing CXCL12, media containing CXCL12 and a specific CXCR4 antagonist or media with a specific CXCR4 antagonist alone for 24 h at 37 °C. Subsequently, cell death was assessed by trypan blue staining (**a**). Staining with Annexin V and 7-AAD was also performed to detect early apoptotic (Annexin $V^+7\text{-}AAD^-$; **b**, **c**) cells and late apoptotic/necrotic (Annexin $V^+7\text{-}AAD^+$; **b**, **d**) cells. Representative dot plots are shown. A total of six mice were used in each group. The values represent mean±s.e.m. $^*P<0.01$ versus before culture group and $^\dagger P<0.01$ versus media only group using ANOVA with Scheffé's *post hoc* test. 7-AAD, 7-aminoactinomycin D; FCS, fetal calf serum.

hematopoietic cells[32] and blood neutrophils of Warts, hypogammaglobulinemia, infections, and myelokathexis syndrome (an inherited immune disorder associated with CXCR4 gene mutation, causing a defect of CXCR4 internalization) patients[34] *via* ERK1/2 and/or PI3K/Akt signaling pathway. Western blotting revealed that CXCL12 induced phosphorylation of both ERK1/2 and Akt (Figure 5a) in the neutrophils isolated from the injured lungs. Moreover, the protective effect of CXCL12 against spontaneous apoptosis on the neutrophils was suppressed by the presence of MEK1/2 inhibitor or PI3K inhibitor (Figure 5b and c). These findings suggested the protective effect of CXCL12/CXCR4 against cell death of the neutrophils accumulated in the lungs during LPS-induced lung injury through ERK and PI3K/Akt signaling pathways.

L-selectin may be involved in the increase in surface CXCR4 expression on neutrophils

Our findings suggested that the increase in surface CXCR4 expression levels occurred during or after the extravasation of neutrophils in the lungs during LPS-induced lung injury. Circulating neutrophils expressed L-selectin on their surface (Figure 6a), whereas significant levels of surface L-selectin expression were not observed on neutrophils in lung digests and BAL fluids during LPS-induced lung injury (Figure 6b and c). These findings suggested that the shedding of L-selectin occurred in the process of extravasation of neutrophils into the injured lungs. To elucidate the participation of L-selectin in the increase in surface CXCR4 expression on neutrophils, we stimulated circulating neutrophils *ex vivo* with sulfatide, one of the native

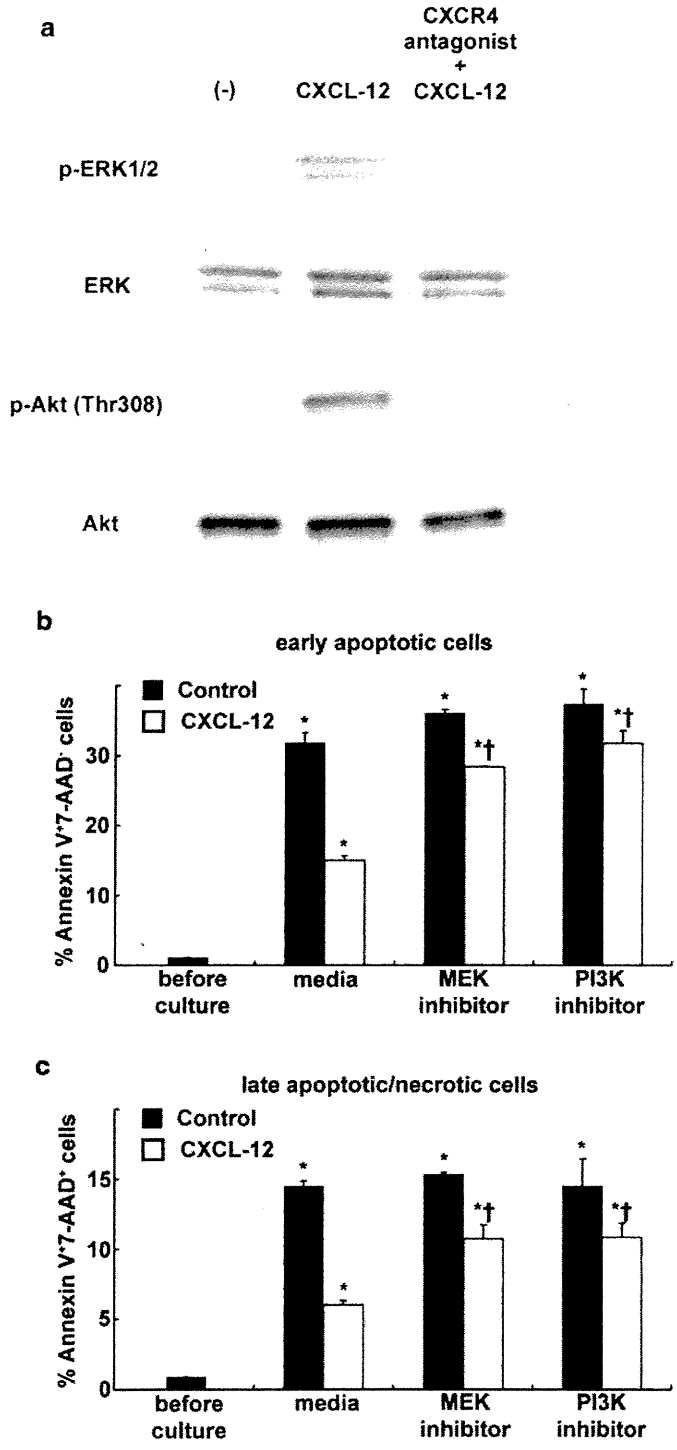

Figure 5 CXCL12 protects lung-accumulated neutrophils of LPS-injured mice from apoptosis through MEK/ERK and PI3K/Akt pathways. (**a**) Neutrophils were isolated from the mouse lungs at 24 h after LPS instillation. Isolated neutrophils were untreated or pre-incubated with a CXCR4 antagonist then treated CXCL12. Western blot analysis showed that CXCL12 induced the phosphorylation of ERK1/2 and Akt. (**b**, **c**) The isolated neutrophils were cultured for 24 h at 37 °C in the presence (white bar) or absence (black bar) of CXCL12 alone or in combination with a MEK1/2 inhibitor (U0126) or a PI3K inhibitor (LY294002). Subsequently, staining with Annexin V and 7-AAD was also performed to detect early apoptotic (Annexin $V^+7\text{-}AAD^-$; **b**) cells and late apoptotic/necrotic (Annexin $V^+7\text{-}AAD^+$; **c**) cells. Note the suppression of the inhibitory effect of CXCL12 against apoptosis in the presence of MEK1/2 inhibitor or PI3K inhibitor. The values represent mean±s.e.m. (n=6). *P<0.01 versus before culture group and $^\dagger P$<0.01 versus media only group using ANOVA with Scheffé's *post hoc* test. 7-AAD, 7-aminoactinomycin D; LPS, lipopolysaccharide.

L-selectin ligands,[35] and examined the changes in CXCR4 expression. Sulfatide induced a significant increase in surface CXCR4 expression on neutrophils (Figure 6d–f) and shedding of L-selectin (Figure 6g and h). This finding suggested that L-selectin may be involved in the increase in surface CXCR4 expression on neutrophils after the emigration of these cells into the injured lungs.

DISCUSSION

In the present study, we demonstrated that cell surface CXCR4 expression levels increase on extravascular neutrophils, but not on intravascular neutrophils, in the injured lung during LPS-induced lung injury. Because CXCL12 is also upregulated in the injured lungs,[17–19] these findings suggest that the increase in surface CXCR4 expression levels on extravasated neutrophils acts together with the increase of CXCL12 in the lungs to promote neutrophil migration and/or retention within the airspace.

To investigate whether the CXCL12/CXCR4 signaling system contributes to neutrophil migration to the lung or retention in the injured lung, we examined the migratory activities of neutrophils isolated from the bone marrow, blood, lung digests and BAL fluids of LPS-injured mice toward CXCL12. Our findings revealed that neutrophils isolated from lung digests and BAL fluids exhibited enhanced migratory activities toward CXCL12, whereas neutrophils isolated from bone marrow or blood did not. These findings were consistent with the low levels of surface CXCR4 expression found on neutrophils isolated from bone marrow and blood (Figure 1a and b). These data suggest that the neutrophils that were accumulated in the lung acquired the ability to migrate toward CXCL12 through the increase in CXCR4 and that the CXCL12/CXCR4 signaling pathway contributes primarily to neutrophil retention, not migration, in cases of LPS-induced lung injury.

We examined whether CXCR4 activation by CXCL12 prevented cell death of lung neutrophils, because the apoptosis of neutrophils and subsequent macrophage phagocytosis of apoptotic cells contribute to neutrophil clearance. We found that CXCL12 reduced the levels of cell death of the extravasated neutrophils within the injured lungs. This protective effect was inhibited when a specific CXCR4 antagonist was administered. We investigated the mechanisms for how CXCL12/CXCR4 signaling protects the lung accumulated neutrophils and then revealed that CXCL12 protects the neutrophils from apoptosis through MEK/ERK and PI3K/Akt pathways. Although we do not have clear evidence confirming that CXCR4 activation is critical for the survival of accumulated neutrophils *in vivo*, this idea is compatible with a recent clinical report describing increased CXCL12 concentrations and the presence of primarily non-apoptotic neutrophils with enhanced CXCR4 expression levels in the BAL fluid of lipopolysaccharide patients.[36] Taken together, our *ex vivo* findings suggest that this protective effect of the CXCL12/CXCR4 signaling pathway against cell death contributes to neutrophil accumulation and retention in the lungs during inflammatory diseases, including cases of acute lung injury.

To investigate the stimuli that induce the increase in surface CXCR4 expression on neutrophils, we focused on L-selectin, a cell adhesion molecule that belongs to the selectin family, because it has been also reported that L-selectin is involved in the increase in surface CXCR4 expression on human peripheral blood lymphocytes and mouse

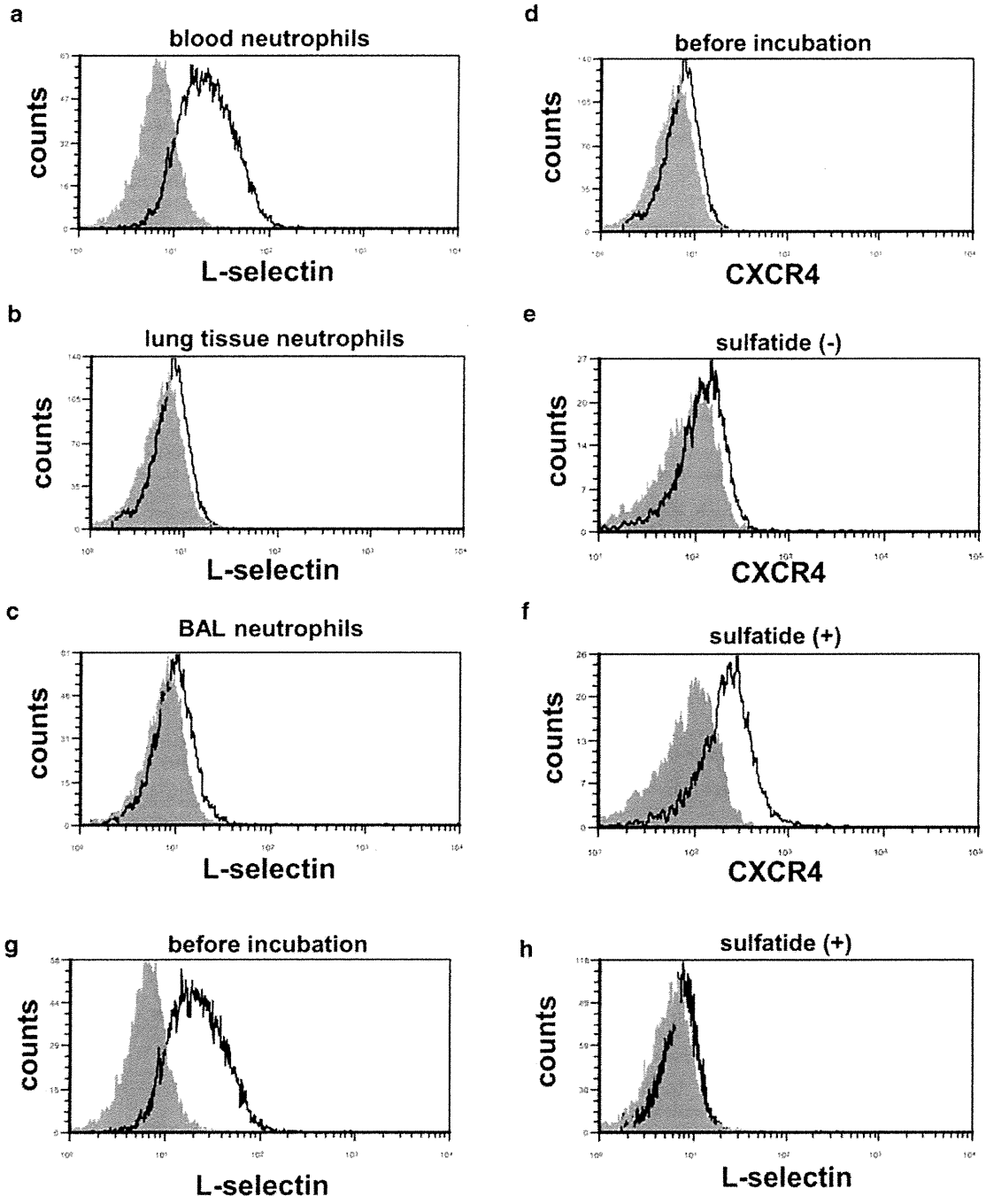

Figure 6 L-selectin may be involved in the increase in surface CXCR4 expression in mouse neutrophils. (**a–c**) The surface L-selectin expression levels of neutrophils isolated from blood (**a**), lung tissue (**b**) and BAL fluid (**c**) at 24 h during LPS-induced lung injury were assessed by flow cytometry. The filled images show the staining using an isotype-matched control antibody. (**d–f**) Sulfatide induced the increase in surface CXCR4 expression in neutrophils isolated from mouse blood. The surface CXCR4 expression levels were examined before incubation (**d**) and after incubation for 1 h either with (**f**) or without (**e**) sulfatide. (**g**, **h**) Sulfatide induced shedding of L-selectin on neutrophils. Surface expressions of L-selectin on neutrophils were examined before incubation (**g**) and after incubation for 1 h with sulfatide (**h**). Representative histograms from one of three experiments that showed similar results are presented. BAL, bronchoalveolar lavage; LPS, lipopolysaccharide.

lymphocytes.[20,21] We observed that the shedding of L-selectin, which is induced by L-selectin activation, occurred during the process of extravasation of neutrophils (Figure 6a–c). We also found that sulfatide, a natural ligand for L-selectin, induced the surface expression of CXCR4 on neutrophils isolated from mouse blood. These findings suggest that the activation of L-selectin may be involved in the increase in surface CXCR4 expression levels on neutrophils in the lungs.

In summary, we have shown that the surface CXCR4 expression levels on neutrophils increase after extravasation into the mouse lungs during LPS-induced lung injury. In addition, the activation of L-selectin may be a key regulator of this surface CXCR4 increase. Our findings suggest that the CXCL12/CXCR4 signaling pathway is involved in neutrophil accumulation and retention in the inflammatory site through both its chemotactic effect and its protective effect against cell death.

Supplementary information accompanies the paper on Cellular & Molecular Immunology's website (http://www.nature.com/cmi/)

ACKNOWLEDGEMENTS

This work was supported by grants from the Japanese Society for the Promotion of Science (no. 17590776 to HK and no. 17790524 to MY). The authors declare no financial or commercial conflict of interest.

1 Kubo H, Graham L, Doyle NA, Quinlan WM, Hogg JC, Doerschuk CM. Complement fragment-induced release of neutrophils from bone marrow and sequestration within pulmonary capillaries in rabbits. *Blood* 1998; **92**: 283–290.
2 Kubo H, Morgenstern D, Quinian WM, Ward PA, Dinauer MC, Doerschuk CM. Preservation of complement-induced lung injury in mice with deficiency of NADPH oxidase. *J Clin Invest* 1996; **97**: 2680–2684.
3 Strieter RM, Kunkel SL, Bone RC. Role of tumor necrosis factor-alpha in disease states and inflammation. *Crit Care Med* 1993; **21**: S447–S463.
4 Gabay C, Lamacchia C, Palmer G. IL-1 pathways in inflammation and human diseases. *Nat Rev Rheumatol* 2010; **6**: 232–241.
5 Romagnani P, Lasagni L, Annunziato F, Serio M, Romagnani S. CXC chemokines: the regulatory link between inflammation and angiogenesis. *Trends Immunol* 2004; **25**: 201–209.
6 Harada A, Sekido N, Akahoshi T, Wada T, Mukaida N, Matsushima K. Essential involvement of interleukin-8 (IL-8) in acute inflammation. *J Leukoc Biol* 1994; **56**: 559–564.
7 Zachariae CO. Chemotactic cytokines and inflammation. Biological properties of the lymphocyte and monocyte chemotactic factors ELCF, MCAF and IL-8. *Acta Derm Venereol Suppl (Stockh)* 1993; **181**: 1–37.
8 Bleul CC, Farzan M, Choe H, Parolin C, Clark-Lewis I, Sodroski J *et al.* The lymphocyte chemoattractant SDF-1 is a ligand for LESTR/fusin and blocks HIV-1 entry. *Nature* 1996; **382**: 829–833.
9 Bleul CC, Fuhlbrigge RC, Casasnovas JM, Aiuti A, Springer TA. A highly efficacious lymphocyte chemoattractant, stromal cell-derived factor 1 (SDF-1). *J Exp Med* 1996; **184**: 1101–1109.
10 Nagasawa T, Nakajima T, Tachibana K, Iizasa H, Bleul CC, Yoshie O *et al.* Molecular cloning and characterization of a murine pre-B-cell growth-stimulating factor/stromal cell-derived factor 1 receptor, a murine homolog of the human immunodeficiency virus 1 entry coreceptor fusin. *Proc Natl Acad Sci USA* 1996; **93**: 14726–14729.
11 Oberlin E, Amara A, Bachelerie F, Bessia C, Virelizier JL, Arenzana-Seisdedos F *et al.* The CXC chemokine SDF-1 is the ligand for LESTR/fusin and prevents infection by T-cell-line-adapted HIV-1. *Nature* 1996; **382**: 833–835.
12 Liles WC, Broxmeyer HE, Rodger E, Wood B, Hubel K, Cooper S *et al.* Mobilization of hematopoietic progenitor cells in healthy volunteers by AMD3100, a CXCR4 antagonist. *Blood* 2003; **102**: 2728–2730.
13 Broxmeyer HE, Orschell CM, Clapp DW, Hangoc G, Cooper S, Plett PA *et al.* Rapid mobilization of murine and human hematopoietic stem and progenitor cells with AMD3100, a CXCR4 antagonist. *J Exp Med* 2005; **201**: 1307–1318.
14 Eash KJ, Means JM, White DW, Link DC. CXCR4 is a key regulator of neutrophil release from the bone marrow under basal and stress granulopoiesis conditions. *Blood* 2009; **113**: 4711–4719.
15 Suratt BT, Petty JM, Young SK, Malcolm KC, Lieber JG, Nick JA *et al.* Role of the CXCR4/SDF-1 chemokine axis in circulating neutrophil homeostasis. *Blood* 2004; **104**: 565–571.
16 Martin C, Burdon PC, Bridger G, Gutierrez-Ramos JC, Williams TJ, Rankin SM. Chemokines acting *via* CXCR2 and CXCR4 control the release of neutrophils from the bone marrow and their return following senescence. *Immunity* 2003; **19**: 583–593.
17 Petty JM, Sueblinvong V, Lenox CC, Jones CC, Cosgrove GP, Cool CD *et al.* Pulmonary stromal-derived factor-1 expression and effect on neutrophil recruitment during acute lung injury. *J Immunol* 2007; **178**: 8148–8157.
18 Yamada M, Kubo H, Kobayashi S, Ishizawa K, Sasaki H. Stromal cell-derived factor-1 contributes to lipopolysaccharide-induced lung injury. *Am J Respir Crit Care Med* 2004; **169**: A875.
19 Yamada M, Kubo H, Kobayashi S, Ishizawa K, Sasaki H. Stromal cell-derived factor-1 contributes to lipopolysaccharide-induced neutrophil emigration within the airspace. *Proc Am Thorac Soc* 2005; **2**: A350.
20 Duchesneau P, Gallagher E, Walcheck B, Waddell TK. Up-regulation of leukocyte CXCR4 expression by sulfatide: an L-selectin-dependent pathway on CD4$^+$ T cells. *Eur J Immunol* 2007; **37**: 2949–2960.
21 Ding Z, Issekutz TB, Downey GP, Waddell TK. L-selectin stimulation enhances functional expression of surface CXCR4 in lymphocytes: implications for cellular activation during adhesion and migration. *Blood* 2003; **101**: 4245–4252.
22 Palecanda A, Walcheck B, Bishop DK, Jutila MA. Rapid activation-independent shedding of leukocyte L-selectin induced by cross-linking of the surface antigen. *Eur J Immunol* 1992; **22**: 1279–1286.
23 Kishimoto TK, Jutila MA, Berg EL, Butcher EC. Neutrophil Mac-1 and MEL-14 adhesion proteins inversely regulated by chemotactic factors. *Science* 1989; **245**: 1238–1241.
24 Jutila MA, Berg EL, Kishimoto TK, Picker LJ, Bargatze RF, Bishop DK *et al.* Inflammation-induced endothelial cell adhesion to lymphocytes, neutrophils, and monocytes. Role of homing receptors and other adhesion molecules. *Transplantation* 1989; **48**: 727–731.
25 Fujii N, Nakashima H, Tamamura H. The therapeutic potential of CXCR4 antagonists in the treatment of HIV. *Expert Opin Investig Drugs* 2003; **12**: 185–195.
26 Tamamura H, Hiramatsu K, Mizumoto M, Ueda S, Kusano S, Terakubo S *et al.* Enhancement of the T140-based pharmacophores leads to the development of more potent and bio-stable CXCR4 antagonists. *Org Biomol Chem* 2003; **1**: 3663–3669.
27 Reutershan J, Basit A, Galkina EV, Ley K. Sequential recruitment of neutrophils into lung and bronchoalveolar lavage fluid in LPS-induced acute lung injury. *Am J Physiol Lung Cell Mol Physiol* 2005; **289**: L807–L815.
28 Tamamura H, Fujisawa M, Hiramatsu K, Mizumoto M, Nakashima H, Yamamoto N *et al.* Identification of a CXCR4 antagonist, a T140 analog, as an anti-rheumatoid arthritis agent. *FEBS Lett* 2004; **569**: 99–104.
29 Matute-Bello G, Winn RK, Jonas M, Chi EY, Martin TR, Liles WC. Fas (CD95) induces alveolar epithelial cell apoptosis *in vivo* implications for acute pulmonary inflammation. *Am J Pathol* 2001; **158**: 153–161.
30 Hendrix CW, Flexner C, MacFarland RT, Giandomenico C, Fuchs EJ, Redpath E *et al.* Pharmacokinetics and safety of AMD-3100, a novel antagonist of the CXCR-4 chemokine receptor, in human volunteers. *Antimicrob Agents Chemother* 2000; **44**: 1667–1673.
31 Hubel K, Liles WC, Broxmeyer HE, Rodger E, Wood B, Cooper S *et al.* Leukocytosis and mobilization of CD34$^+$ hematopoietic progenitor cells by AMD3100, a CXCR4 antagonist. *Support Cancer Ther* 2004; **1**: 165–172.
32 Lataillade JJ, Clay D, Bourin P, Herodin F, Dupuy C, Jasmin C *et al.* Stromal cell-derived factor 1 regulates primitive hematopoiesis by suppressing apoptosis and by promoting G_0/G_1 transition in CD34$^+$ cells: evidence for an autocrine/paracrine mechanism. *Blood* 2002; **99**: 1117–1129.
33 Vlahakis SR, Villasis-Keever A, Gomez T, Vanegas M, Vlahakis N, Paya CV. G protein-coupled chemokine receptors induce both survival and apoptotic signaling pathways. *J Immunol* 2002; **169**: 5546–5554.
34 Sanmun D, Garwicz D, Smith CI, Palmblad J, Fadeel B. Stromal-derived factor-1 abolishes constitutive apoptosis of WHIM syndrome neutrophils harbouring a truncating CXCR4 mutation. *Br J Haematol* 2006; **134**: 640–644.
35 Suzuki Y, Toda Y, Tamatani T, Watanabe T, Suzuki T, Nakao T *et al.* Sulfated glycolipids are ligands for a lymphocyte homing receptor, L-selectin (LECAM-1), binding epitope in sulfated sugar chain. *Biochem Biophys Res Commun* 1993; **190**: 426–434.
36 Hartl D, Krauss-Etschmann S, Koller B, Hordijk PL, Kuijpers TW, Hoffmann F *et al.* Infiltrated neutrophils acquire novel chemokine receptor expression and chemokine responsiveness in chronic inflammatory lung diseases. *J Immunol* 2008; **181**: 8053–8067.

DOI: 10.1002/cmdc.201100542

A Synthetic C34 Trimer of HIV-1 gp41 Shows Significant Increase in Inhibition Potency

Wataru Nomura,[a] Chie Hashimoto,[a] Aki Ohya,[a] Kosuke Miyauchi,[b] Emiko Urano,[b] Tomohiro Tanaka,[a] Tetsuo Narumi,[a] Toru Nakahara,[a] Jun A. Komano,[b] Naoki Yamamoto,[c] and Hirokazu Tamamura*[a]

The development of new anti-HIV-1 drugs such as inhibitors of protease and integrase has been contributed to highly active anti-retroviral therapy (HAART) for the treatment of AIDS.[1] The entry of human immunodeficiency virus type 1 (HIV-1) into target cells is mediated by its envelope glycoprotein (Env), a type I transmembrane protein that consists of surface subunit gp120 and noncovalently associated transmembrane subunit gp41.[2] Sequential binding of HIV-1 gp120 to its cell receptor CD4 and a co-receptor (CCR5 or CXCR4) can trigger a series of conformational rearrangements in gp41 to mediate fusion between viral and cellular membranes.[3–5] The protein gp41 is hidden beneath gp120, and its ectodomain contains helical N- and C-terminal leucine/isoleucine heptad repeat domains, N-HR and C-HR. Particular regions of N-HR and C-HR are involved in membrane fusion, and 36-mer and 34-mer peptides, which are derived from N-HR and C-HR, have been designated as the N-terminal helix (N36) and C-terminal helix (C34), respectively. In the membrane fusion of HIV-1, these helices assemble to form a six-helical bundle (6-HB) consisting of a central parallel trimer of N36 surrounded by C34 in an antiparallel hairpin fashion. Synthetic peptides derived from these helices have potent antiviral activity against both laboratory-adapted strains and primary isolates of HIV-1.[6–9] They inhibit the membrane fusion stage of HIV-1 infection in a dominant-negative manner by binding to the counterpart regions of gp41 (N-HR or C-HR), blocking formation of the viral gp41 core.

Several potent anti-HIV-1 peptides based on the C-HR region have been discovered,[7,8] and T20 was subsequently developed as the clinical anti-HIV-1 drug enfuvirtide (Roche/Trimeris).[8,10–13] It is a 36-mer peptide derived from the gp41 C-HR sequence and can bind to the N-HR to prevent formation of the 6-HB in a dominant-negative fashion.[10] T20 therapy has brought safety, potent antiretroviral activity, and immunological benefit to patients, but its clinical application is limited by the development of resistance. The C-terminal helix C34 is also a C-HR-derived peptide, and contains the amino acid residues required for docking into the hydrophobic pocket, termed the "deep pocket", of the trimer of the N-HR region. This peptide potently inhibits HIV-1 fusion in vitro.[14] To date, several gp41 mimetics, especially those of N36 regions, which assemble these helical peptides with branched peptide linkers, have been synthesized as antigens.[15–19]

Recently, by using a novel template with C3-symmetric linkers of equal length, we synthesized a three-helix bundle mimetic that corresponds to the trimeric form of N36.[20] The antisera obtained from mice immunized by the peptide antigen showed strong recognition against the N36 trimer peptide with structural preference. At the same time, the trimer peptide was also investigated as a fusion inhibitor. However, the trimer N36 showed only a threefold increase in inhibition of HIV-1 fusion relative to the N36 monomer.[20] In terms of N36 content, the trimer and monomer have nearly the same inhibitory potency. This phenomenon is consistent with the results from other studies.[21–23] The multimerization of the functional unit, such as synthetic ligands against receptors, show synergistic binding and strong binding activity. Thus, we hypothesized that our strategy using C3-symmetric linkers in the design of trimer mimics of gp41 could be applied to the C34 peptide, which shows significant inhibition potency in the monomeric form. In the present study, we designed and synthesized a novel three-helical bundle structure of the trimeric form of C34. This equivalent mimic of the trimeric form of C34 was evaluated as a novel form of fusion inhibitor.

The C-terminal region of gp41 is known to be an assembly site involving a trimeric coiled-coil conformation. In the design of the C34-derived peptides C34REG-thioester (Figure 1A) and C34REG (Figure 1B), the triplet repeat of arginine and glutamic acid (RERERE) was added to the C-terminal end of the C34 sequence (residues 628–661) to increase aqueous solubility, and for C34REG-thioester, a glycine thioester was fused to the C terminus. To form a triple helix corresponding precisely to the gp41 pre-fusion form, we designed the novel C3-symmetric template depicted in Figure 1C. This designed template linker has three branches of equal length, a hydrophilic structure, and a ligation site for coupling with C34REG-thioester. The template was synthesized as shown in Scheme 1. This approach uses native chemical ligation for chemoselective coupling of unprotected C34REG-thioester with a three-armed cysteine scaffold to produce triC34e (Figure 2).[24,25]

Circular dichroism (CD) spectra of C34REG and triC34e are shown in Figure 3A. The peptides were dissolved in 50 mM sodium phosphate buffer with 150 mM NaCl, pH 7.2. Both spectra display minima at ~200 nm, indicating that these peptides form random structures. We previously reported that the

[a] Dr. W. Nomura, C. Hashimoto, A. Ohya, Dr. T. Tanaka, Dr. T. Narumi, T. Nakahara, Prof. Dr. H. Tamamura
Institute of Biomaterials and Bioengineering
Tokyo Medical and Dental University
2-3-10 Kandasurugadai, Chiyoda-ku, Tokyo 101-0062 (Japan)
E-mail: tamamura.mr@tmd.ac.jp

[b] Dr. K. Miyauchi, Dr. E. Urano, Dr. J. A. Komano
AIDS Research Center, National Institute of Infectious Diseases
1-23-1 Toyama, Shinjuku-ku, Tokyo 162-8640 (Japan)

[c] Prof. Dr. N. Yamamoto
Department of Microbiology, Yong Loo Lin School of Medicine
National University of Singapore
5 Science Drive 2, Singapore 117597 (Singapore)

Supporting information for this article is available on the WWW under http://dx.doi.org/10.1002/cmdc.201100542.

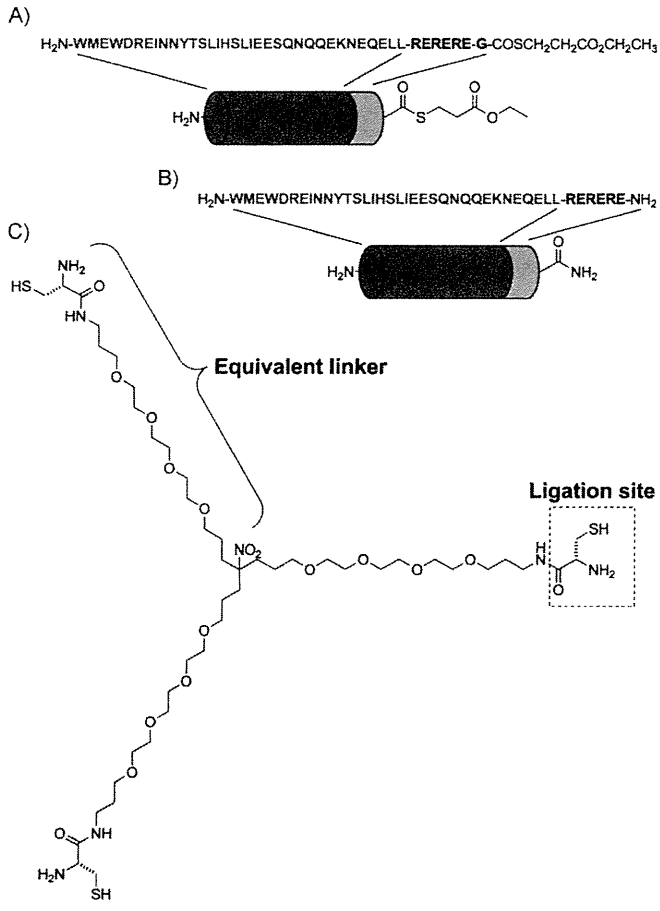

Figure 1. C34-derived peptides: A) C34REG-thioester and B) C34REG. C) The design of a C3-symmetric template.

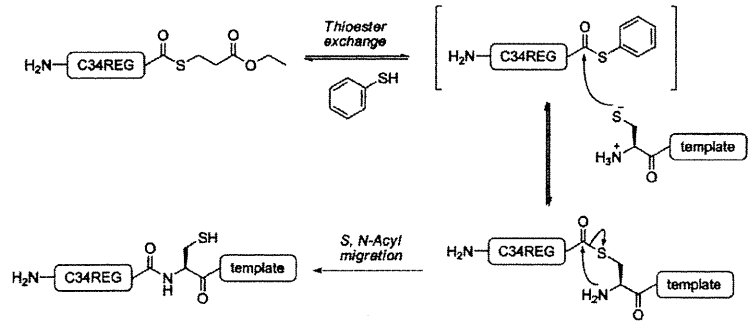

Figure 2. The native chemical ligation used for assembly of the C34REG-thioester on the template.

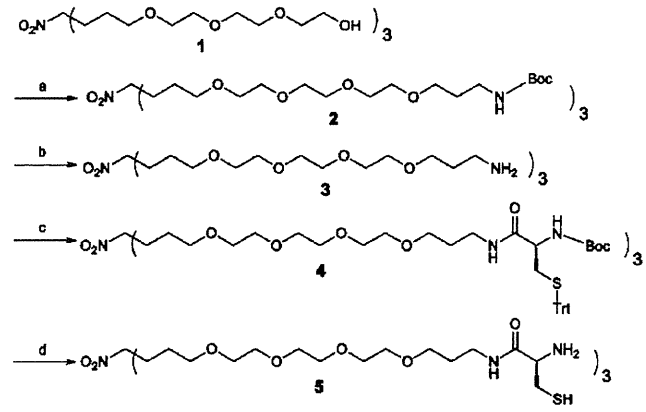

Scheme 1. Synthesis of the equivalently branched template **5**. *Reagents and conditions*: a) (3-bromopropyl)carbamic acid *tert*-butyl ester, NaH, THF; b) 4 M HCl/dioxane; c) Boc-Cys(Trt)-OH, EDCI·HCl, HOBt·H_2O, Et_3N, DMF; d) 90% aq. TFA.

helical content of the trimer triC34e and N36RE mixture is lower than that of the monomer C34REG and N36RE mixture. This is evidence that relative to the monomer C34REG, the trimer triC34e interacts with N36 only with difficulty, due to the assembly of three peptide strands by covalent bonds.

As the trimeric C34 was proven to interact with N36 helices, the potential HIV-1 inhibitory activities of the C-terminal peptides, C34REG and triC34e, were evaluated. The C34 peptide without the solubility-increasing sequence (3×[Arg-Glu], obtained from NIAID) was used as the monomeric control.[27] All peptides showed potent inhibitory activity in the viral fusion assay (Table 1), with the potency of triC34e being 100- and 40-fold higher than that of C34REG and C34 peptides, respectively. Notably, the triC34e trimer peptide is remarkably more potent in anti-HIV-1 activity than the monomer, indicating that a trimeric form is critical for inhibitory activity. Cytotoxicity from the peptides was not observed at concentrations of 15 μM for C34REG and C34, and 5 μM for triC34e.

We next carried out an assay for the inhibition of viral replication. As shown in Table 2, triC34e showed 30- and 20-fold higher inhibitory activity than peptides C34 and C34REG, respectively. In the two anti-HIV-1 assays, triC34e showed a great enhancement of activity over the C34 monomers. The IC_{50} values obtained in the assays are different, and this can be

N36 monomer N36RE and the N36 trimer triN36e form a highly structured α helix, and that the helical content of triN36e was greater than that of N36RE.[20,26] These results suggest that in contrast to N36-derived peptides, C34-derived peptides tend to form random structures both in the monomeric and trimeric forms. To assess the interaction of triC34e with N36, CD spectra of a mixture of triC34e with an N36-derived peptide, N36RE, were measured (Figure 3 B). The spectrum of the C34REG and N36RE mixture and that of the triC34e and N36RE mixture showed double minima at λ 208 and 222 nm, indicating that the peptide mixture forms an α-helical structure and that the

Table 1. IC_{50} and CC_{50} values determined by viral fusion inhibition and cell viability assays.

	C34 peptide[a]	C34REG	triC34e
IC_{50} [μM][b]	0.044	0.12	0.0013
CC_{50} [μM][c]	>15	>15	>5

[a] HIV-1 IIIB C34 peptide. [b] IC_{50} values are based on luciferase signals in TZM-bl cells infected with HIV-1 (NL4-3 strain). [c] CC_{50} values are based on the decrease in viability of TZM-bl cells. All data are the mean values from at least three experiments.

Table 2. IC_{50} values determined by inhibition assay based on p24 ELISA.

	C34 peptide	C34REG	triC34e
IC_{50} [μM][a]	1.59	1.06	0.0547

[a] IC_{50} values are based on the production of p24 in MT-4 cells infected with HIV-1 (NL4-3 strain). All data are the mean values from at least three experiments.

explained through differences in experimental procedures. In the fusion inhibition assay, cells were treated with peptides before viral infection. In contrast, in the viral replication inhibition assay, peptides were treated after viral adsorption to cells. Therefore, in the latter case, the infection by HIV-1 might precede peptide binding to gp41.

It has been shown that T-1249, an analogue of enfuvirtide, and its hydrophobic C-terminal region inhibit HIV-1 fusion by interacting with lipid bilayers.[28] The tryptophan-rich domain of T-1249 was shown to play important roles in HIV-1 fusion.[29–31] As enfuvirtide shows weak interaction with the gp41 core structure, and the C34 sequence lacks the C-terminal lipid binding domain, it has been suggested that C34 has a mechanism of action distinct from that of enfuvirtide.[32] Thus, it is of interest to discern the mechanism of the enhanced inhibition observed with triC34e relative to the monomer. Two explanations can be envisaged: 1) the α helicity of the C34 trimer is higher than that of the monomer, as shown in Figure 3A, and as a result, the C34 trimer binds more strongly to the N36 trimer; and 2) in the mixture with the N36 monomer, the C34 trimer shows less α helicity than its monomer (Figure 3B). As shown in Figure 3A, the molar ellipticity at 222 nm is similar for both the C34 trimer and the monomer. Thus, the decrease at 222 nm in the mixture with N36 might be due to a decrease in the α helicity of N36. These results suggest that the C34 trimer might destabilize helix formation in N36 and thus exert potent inhibitory activity. It has been shown that a dimeric C37 (residues 625–661) variant does not show a significant difference in IC_{50} value against HIV-1 from wild-type C37, although the dimeric peptide shows tighter binding to the gp41 N-HR coiled-coil than the C37 monomer.[33] Thus, the mechanism of action of the C34 trimer could be different from that of the dimeric C-peptide. The detailed action mechanism of the trimer as a fusion inhibitor and the reasons behind its remarkable increased anti-HIV-1 activity will be the subjects of future studies in our research group.

A C-terminal helical peptide of HIV-1 gp41 has been designed as a new HIV fusion inhibitor and was synthesized with a novel template and three branched linkers of equal length. The native chemical ligation proceeded by chemoselective coupling in an aqueous medium of an unprotected C34 derivative containing a C-terminal thioester with a three-cysteine-armed scaffold. This process led to the production of triC34e. As a fusion inhibitor, triC34e has potent anti-HIV-1 activity, 100-fold greater than that of the C34REG monomer, although the anti-HIV-1 activity of the N36 trimer is threefold higher than that of the N36 monomer, and the N36 content is the same in both cases.[20] A trimeric form of C34 is evidently critical as the

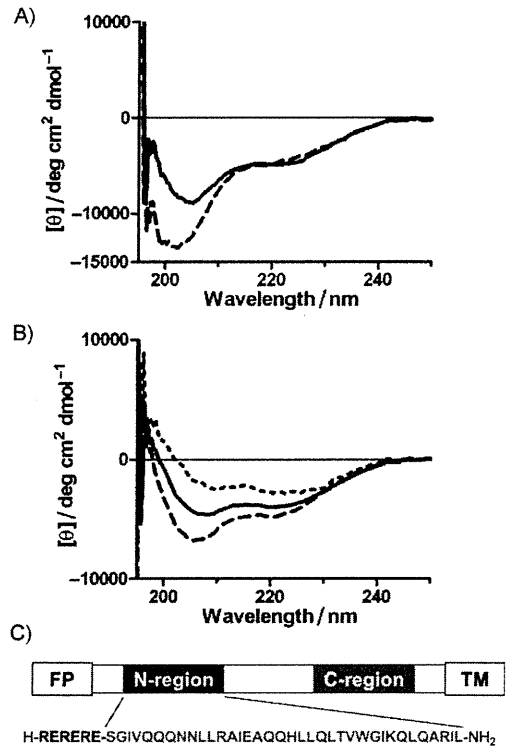

Figure 3. A) CD spectra of C34REG (monomer, -----, 6 μM) and triC34e (trimer, ——, 2 μM). B) CD spectra in the presence or absence of the N36 monomer N36RE:[20] -----, [C34REG (6 μM) + N36RE (6 μM)]; ——, [triC34e (2 μM) + N36RE (6 μM)]; ••••, N36RE (6 μM). In the amino acid sequence of N36RE, the triplet repeat of arginine and glutamic acid is located at the N-terminus of the original N36 sequence.[20] C) Amino acid sequence of N36RE: FP and TM represent the hydrophobic fusion peptide and transmembrane domains, respectively.

active structure of the fusion inhibitor. The soluble C34 derivative, SC34, retains potent inhibitory effects against enfuvirtide-resistant viruses,[34] and this suggests that the present highly potent trimeric inhibitor could be effective for enfuvirtide-resistant HIV-1 strains. The design of inhibitors that target the dynamic supramolecular mechanism of HIV-1 fusion will be useful for future studies of anti-HIV-1 agents.

Experimental Section

Conjugation of C34REG-thioester and the template to produce triC34e

TCEP·HCl (773 μg, 2.67 μmol) and thiophenol (9 μL, 89 μmol) were dissolved in 0.1 M sodium phosphate buffer (60 μL) containing 6 M urea and EDTA (pH 8.5, 2 mM) under a nitrogen atmosphere. Compound **5** (100 μg, 0.0899 μmol), C34REG-thioester (1.77 mg, 0.297 μmol), and CH_3CN (20 μL) were added. The reaction was stirred for 5 h at 37 °C and monitored by HPLC. The ligation product (triC34e) was separated as an HPLC peak and characterized by ESI-ToF-MS (*m/z* calcd for $C_{703}H_{1108}N_{205}O_{245}S_6$ $[M+H]^+$: 16533.9, found: 16543.8). Purification was performed by reversed-phase HPLC (Cosmosil 5 C_{18}-AR II column, 10×250 mm, Nacalai Tesque, Inc.) with elution using a 33–43% linear gradient of CH_3CN (0.1% TFA) over 40 min. Purified triC34e, obtained in 17% yield, was identified by ESI-ToF-MS. Details of the synthesis of these peptides are described in the Supporting Information.

CD spectra

Circular dichroism measurements were performed with a J-720 CD spectropolarimeter equipped with a thermoregulator (Jasco). The wavelength dependence of molar ellipticity [θ] was monitored at 25 °C from λ 195 to 250 nm. The peptides were dissolved in PBS (50 mM sodium phosphate, 150 mM NaCl, pH 7.2).

Virus preparation

For virus preparation, 293FT cells in a 60 mm dish were transfected with the pNL4-3 construct (10 μg) by the calcium phosphate method. The supernatant was collected 48 h after transfection, passed through a 0.45 μm filter, and stored at −80 °C as the virus stock.

Anti-HIV-1 assay

For the viral fusion inhibition assay, TZM-bl cells (2×10^4 cells per 100 μL) were cultured with the NL4-3 virus (5 ng of p24) and serially diluted peptides. After culture for 48 h, cells were lysed, and the luciferase activity was determined with the Steady-Glo luciferase assay system (Promega, Fitchburg, WI, USA).[35] For the viral replication inhibition assay, MT-4 cells (5×10^4 cells) were exposed to HIV-1 NL4-3 (1 ng of p24) at 4 °C for 30 min. After centrifugation, cells were resuspended with 150 μL medium containing indicated concentrations of serially diluted peptides. Cells were cultured at 37 °C for 3 days, and the concentration of p24 in the culture supernatant was determined by HIV-1 p24 antigen ELISA kit (ZeptoMetrix, Buffalo, NY, USA).

Cytotoxicity assay

The cytotoxic effects of peptides were determined by the CellTiter 96 AQueous One Solution Cell Proliferation assay system (Promega) under the same conditions, but in the absence of viral infection.

Acknowledgements

The following reagent was obtained through the US National Institutes of Health (NIH) AIDS Research and Reference Reagent Program, Division of AIDS, NIAID, NIH: HIV-1 IIIB C34 Peptide from DAIDS, NIAID. This work was supported in part by a Grant-in-Aid for Scientific Research from the Ministry of Education, Culture, Sports, Science, and Technology of Japan, and Health and Labour Sciences Research Grants from the Japanese Ministry of Health, Labor, and Welfare. C.H. is supported by JSPS research fellowships for young scientists.

Keywords: antiviral agents · C34 trimers · fusion inhibitors · gp41 · HIV-1

[1] C. Hashimoto, T. Tanaka, T. Narumi, W. Nomura, H. Tamamura, *Expert Opin. Drug Discovery* **2011**, *6*, 1067–1090.
[2] E. O. Freed, M. A. Martin, *J. Biol. Chem.* **1995**, *270*, 23883–23886.
[3] D. M. Eckert, P. S. Kim, *Annu. Rev. Biochem.* **2001**, *70*, 777–810.
[4] R. Wyatt, J. Sodroski, *Science* **1998**, *280*, 1884–1888.
[5] E. A. Berger, P. M. Murphy, J. M. Farber, *Annu. Rev. Immunol.* **1999**, *17*, 657–700.
[6] M. Lu, S. C. Blacklow, P. S. Kim, *Nat. Struct. Biol.* **1995**, *2*, 1075–1082.
[7] S. Jiang, K. Lin, N. Strick, A. R. Neurath, *Nature* **1993**, *365*, 113.
[8] C. T. Wild, D. C. Shugars, T. K. Greenwell, C. B. McDanal, T. J. Matthews, *Proc. Natl. Acad. Sci. USA* **1994**, *91*, 9770–9774.
[9] C. T. Wild, T. Oas, C. McDanal, D. Bolognesi, T. Matthews, *Proc. Natl. Acad. Sci. USA* **1992**, *89*, 10537–10541.
[10] J. M. Kilby, S. Hopkins, T. M. Venetta, B. DiMassimo, G. A. Cloud, J. Y. Lee, L. Alldredge, E. Hunter, D. Lambert, D. Bolognesi, T. Matthews, M. R. Johnson, M. A. Nowak, G. M. Shaw, M. S. Saag, *Nat. Med.* **1998**, *4*, 1302–1307.
[11] J. M. Kilby, J. J. Eron, *N. Engl. J. Med.* **2003**, *348*, 2228–2238.
[12] J. P. Lalezari, K. Henry, M. O'Hearn, J. S. Montaner, P. J. Piliero, B. Trottier, S. Walmsley, C. Cohen, D. R. Kuritzkes, J. J. Eron, Jr., J. Chung, R. DeMasi, L. Donatacci, C. Drobnes, J. Delehanty, M. Salgo, *N. Engl. J. Med.* **2003**, *348*, 2175–2185.
[13] S. Liu, W. Jing, B. Cheng, H. Lu, J. Sun, X. Yan, J. Niu, J. Farmar, S. Wu, S. Jiang, *J. Biol. Chem.* **2007**, *282*, 9612–9620.
[14] D. C. Chan, D. Fass, J. M. Berger, P. S. Kim, *Cell* **1997**, *89*, 263–273.
[15] E. De Rosny, R. Vassell, R. T. Wingfield, C. T. Wild, C. D. Weiss, *J. Virol.* **2001**, *75*, 8859–8863.
[16] J. P. Tam, Q. Yu, *Org. Lett.* **2002**, *4*, 4167–4170.
[17] W. Xu, J. W. Taylor, *Chem. Biol. Drug Des.* **2007**, *70*, 319–328.
[18] J. M. Louis, I. Nesheiwat, L. Chang, G. M. Clore, C. A. Bewlet, *J. Biol. Chem.* **2003**, *278*, 20278–20285.
[19] E. Bianch, J. G. Joyce, M. D. Miller, A. C. Finnefrock, X. Liang, M. Finotto, P. Ingllinella, P. McKenna, M. Citron, E. Ottinger, R. W. Hepler, R. Hrin, D. Nahas, C. Wu, D. Montefiori, J. W. Shiver, A. Pessi, P. S. Kim, *Proc. Natl. Acad. Sci. USA* **2010**, *107*, 10655–10660.
[20] T. Nakahara, W. Nomura, K. Ohba, A. Ohya, T. Tanaka, C. Hashimoto, T. Narumi, T. Murakami, N. Yamamoto, H. Tamamura, *Bioconjugate Chem.* **2010**, *21*, 709–714.
[21] M. Lu, H. Ji, S. Shen, *J. Virol.* **1999**, *73*, 4433–4438.
[22] D. M. Eckert, P. S. Kim, *Proc. Natl. Acad. Sci. USA* **2001**, *98*, 11187–11192.
[23] E. Bianchi, M. Finotto, P. Ingallinella, R. Hrin, A. V. Carella, X. S. Hous, W. A. Schleif, M. D. Miller, *Proc. Natl. Acad. Sci. USA* **2005**, *102*, 12903–12908.
[24] P. E. Dawson, T. W. Muir, I. Clark-Lewis, S. B. H. Kent, *Science* **1994**, *266*, 776–779.
[25] P. E. Dawson, M. J. Churchill, M. R. Ghadiri, S. B. H. Kent, *J. Am. Chem. Soc.* **1997**, *119*, 4325–4329.
[26] D. C. Chan, C. T. Chutkowski, P. S. Kim, *Proc. Natl. Acad. Sci. USA* **1998**, *95*, 15613–15617.
[27] S. A. Gallo, K. Sackett, S. S. Rawat, Y. Shai, R. Blumenthal, *J. Mol. Biol.* **2004**, *340*, 9–14.
[28] A. S. Veiga, N. C. Santos, L. M. Loura, A. Fedorov, M. A. Castanho, *J. Am. Chem. Soc.* **2004**, *126*, 14758–14763.
[29] M. K. Lawless, S. Barney, K. I. Guthrie, T. B. Bucy, S. R. Petteway, Jr., G. Merutka, *Biochemistry* **1996**, *35*, 13697–13708.
[30] K. Salzwedel, J. T. West, E. Hunter, *J. Virol.* **1999**, *73*, 2469–2480.
[31] S. G. Peisajovich, S. A. Gallo, R. Blumenthal, Y. Shai, *J. Biol. Chem.* **2003**, *278*, 21012–21017.
[32] S. Liu, H. Lu, Y. Xu, S. Wu, S. Jiang, *J. Biol. Chem.* **2005**, *280*, 11259–11273.
[33] K. M. Kahle, K. Steger, M. J. Root, *PLoS Pathog.* **2009**, *5*, e1000674.
[34] A. Otaka, M. Nakamura, D. Nameki, E. Kodama, S. Uchiyama, S. Nakamura, H. Nakano, H. Tamamura, Y. Kobayashi, M. Matsuoka, N. Fujii, *Angew. Chem.* **2002**, *114*, 3061–3064; *Angew. Chem. Int. Ed.* **2002**, *41*, 2937–2940.
[35] E. J. Platt, K. Wehrly, S. E. Kuhmann, B. Chesebro, D. Kabat, *J. Virol.* **1998**, *72*, 2855–2864.

Received: November 22, 2011
Revised: December 15, 2011
Published online on January 13, 2012

Bioorganic & Medicinal Chemistry 20 (2012) 1468–1474

Contents lists available at SciVerse ScienceDirect

Bioorganic & Medicinal Chemistry

journal homepage: www.elsevier.com/locate/bmc

Conjugation of cell-penetrating peptides leads to identification of anti-HIV peptides from matrix proteins

Tetsuo Narumi [a], Mao Komoriya [a], Chie Hashimoto [a], Honggui Wu [b,c], Wataru Nomura [a], Shintaro Suzuki [a], Tomohiro Tanaka [a], Joe Chiba [c], Naoki Yamamoto [d], Tsutomu Murakami [b,*], Hirokazu Tamamura [a,*]

[a] Institute of Biomaterials and Bioengineering, Tokyo Medical and Dental University, Chiyoda-ku, Tokyo 101-0062, Japan
[b] AIDS Research Center, National Institute of Infectious Diseases, Shinjuku-ku, Tokyo 162-8640, Japan
[c] Department of Biological Science Technology, Tokyo University of Science, Noda, Chiba 278-8510, Japan
[d] Yong Loo Lin School of Medicine, National University of Singapore, Singapore 117597, Singapore

ARTICLE INFO

Article history:
Received 6 December 2011
Revised 24 December 2011
Accepted 24 December 2011
Available online 2 January 2012

Keywords:
Matrix protein
Octa-arginyl group
Overlapping peptide
Anti-HIV

ABSTRACT

Compounds which inhibit the HIV-1 replication cycle have been found amongst fragment peptides derived from an HIV-1 matrix (MA) protein. Overlapping peptide libraries covering the whole sequence of MA were designed and constructed with the addition of an octa-arginyl group to increase their cell membrane permeability. Imaging experiments with fluorescent-labeled peptides demonstrated these peptides with an octa-arginyl group can penetrate cell membranes. The fusion of an octa-arginyl group was proven to be an efficient way to find active peptides in cells such as HIV-inhibitory peptides.

1. Introduction

Several anti-retroviral drugs beyond reverse transcriptase inhibitors, including effective protease inhibitors[1] and integrase inhibitors[2,3] are currently available to treat human immunodeficiency virus type 1 (HIV-1) infected individuals. We have also developed several anti-HIV agents such as coreceptor CXCR4 antagonists,[4–7] CD4 mimics,[8–10] fusion inhibitors[11] and integrase inhibitors.[12,13] However, the emergence of viral strains with multi-drug resistance (MDR), which accompanies the development of any antiviral drug, has encouraged a search for new types of anti-HIV-1 drugs with different inhibitory mechanisms.

Matrix (MA) proteins are essential for assembly of the virion shell. MA is a component of the Gag precursor protein, Pr55Gag, and is located within the viral membrane.[14,15] It has been reported that MA-derived peptides such as MA(47–59) inhibit infection by HIV,[16] and that MA-derived peptides such as MA(31–45) and MA(41–55) show anti-HIV activity.[17] In addition, Morikawa et al. report that MA(61–75) and MA(71–85) inhibit MA dimerization, a necessary step in the formation of the virion shell.[18] However, the question of whether the above MA peptides can penetrate cell membranes was not addressed in these reports. We speculate that to achieve antiviral activity it is essential that the MA-derived peptides penetrate the cell membrane and function intracellularly. In this paper, we report our design and construction of an overlapping library of fragment peptides derived from the MA protein with a cell membrane permeable signal. Our aim is the discovery of potent lead compounds, which demonstrate HIV inhibitory activity inside the host cells.

2. Materials and methods

2.1. Peptide synthesis

MA-derived fragments and an octa-arginyl (R_8) peptide were synthesized by stepwise elongation techniques of Fmoc-protected amino acids on a Rink amide resin. Coupling reactions were performed using 5.0 equiv of Fmoc-protected amino acid, 5.0 equiv of diisopropylcarbodiimide and 5.0 equiv of 1-hydroxybenzotriazole monohydrate. Ac_2O–pyridine (1/1, v/v) for 20 min was used to acetylate the N-terminus of MA-derived fragments, with the exception of fragment 1. Chloroactylation of the N-terminus of the R_8 peptide, was achieved with 40 equiv of chloroacetic acid, 40 equiv of diisopropylcarbodiimide and 40 equiv of 1-hydroxybenzotriazole monohydrate, treated for 1 h. Cleavage of peptides from resin and side chain deprotection were carried out by stirring for 1.5 h with a mixture of TFA, thioanisole, ethanedithiol, *m*-cresol

* Corresponding authors. Tel.: +81 3 5285 1111; fax: +81 3 5285 5037 (T.M.); tel.: +81 3 5280 8036; fax: +81 3 5280 8039 (H.M.).
E-mail addresses: tmura@nih.go.jp (T. Murakami), tamamura.mr@tmd.ac.jp (H. Tamamura).

0968-0896/$ - see front matter © 2011 Elsevier Ltd. All rights reserved.
doi:10.1016/j.bmc.2011.12.055

and triisopropylsilane (8.15/0.75/0.75/0.25/0.25/0.1, v/v). After removal of the resins by filtration, the filtrate was concentrated under reduced pressure, and crude peptides were precipitated in cooled diethyl ether. All crude peptides were purified by RP-HPLC and identified by ESI-TOFMS. In the conjugation of the R_8 peptide (or iodoacetamide), the peptide (or iodoacetamide) solution in 0.1 M phosphate buffer, pH 7.8 was added to MA fragments which were synthesized as described above. The reaction mixture was stirred at room temperature under nitrogen. After 24 h (or 1 h for the conjugation of iodoacetamide), purification was performed by RP-HPLC. The purified peptides were identified by ESI-TOF MS and lyophilized. Purities of all final compounds were confirmed to be >95% by analytical HPLC. Detailed data are provided in Supplementary data.

2.2. Anti-HIV-1 assay

Anti-HIV-1 (NL4-3 or NL(AD8)) activity was determined by measurement of the protection against HIV-1-induced cytopathogenicity in MT-4 cells or PM1/CCR5 cells. Various concentrations of test peptide solutions were added to HIV-1 infected MT-4 or PM1/CCR5 cells at multiplicity of infection (MOI) of 0.001 and placed in wells of a 96-well microplate. After 5 day incubation at 37 °C in a CO_2 incubator, the number of viable cells was determined using the 3-(4,5-dimethylthiazol-2-yl)-2,5-diphenyltetrazolium bromide (MTT) method. The anti-HIV-1 (JR-CSF) activity was also determined by measuring capsid p24 antigen concentrations of the culture supernatant in the infected cultures by a commercially available ELISA assay (ZeptoMetrix Corp., Buffalo, NY).

2.3. CD spectroscopy

CD spectra were recorded on a JASCO J-720 spectropolarimeter at 25 °C. The measurements were performed using a 0.1 cm path length cuvette at a 0.1 nm spectral resolution. Each spectrum represents the average of 10 scans, and the scan rate was 50 nm/min. The concentrations of samples 8L and 9L were 28.2 and 64.7 μM, respectively, in PBS buffer (pH 7.4).

2.4. Fluorescent imaging of cell-penetrating MA peptides

Cells were seeded on 35 mm glass-bottom dish (2×10^5 cells/dish for HeLa and A549, 1×10^5 cells/dish for CHO-K1) one day before the experiments. The cells were cultured in DMEM/10% FBS/Penicillin–Streptomycin for HeLa and A549, or Ham's F12/10% FBS/Penicillin–Streptomycin for CHO-K1 at 37 °C/5% CO_2. Before the addition of MA peptides, cells were washed with Hanks' balanced salt solutions (HBSS) once. Peptides were added at 5 μM and further cultured for 30 min at 37 °C/5% CO_2. After incubation, cells were washed three times with HBSS and observed under a confocal laser-scanning microscopy (Zeiss LSM510).

3. Results and discussion

An overlapping peptide library spanning the whole sequence of the MA domain, p17, of NL4-3, the Gag precursor Pr55 of HIV-1 was designed. The full sequence of MA consists of 132 amino acid residues. In the peptide library, the MA sequence was divided from the N-terminus in 15-residue segments with an overlap of 5

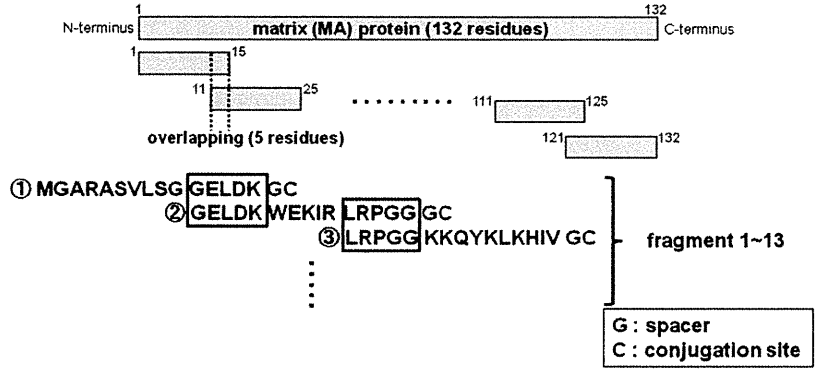

fragment number	sequence
1	H-MGARASVLSGGELDKGC-NH_2
2	CH_3CO-GELDKWEKIRLRPGGGC-NH_2
3	CH_3CO-LRPGGKKQYKLKHIVGC-NH_2
4	CH_3CO-LKHIVWASRELERFAGC-NH_2
5	CH_3CO-LERFAVNPGLLETSEGC-NH_2
6	CH_3CO-LETSEGSRQILGQLQGC-NH_2
7	CH_3CO-LGQLQPSLQTGSEELGC-NH_2
8	CH_3CO-GSEELRSLYNTIAVLGC-NH_2
9	CH_3CO-TIAVLYSVHQRIDVKGC-NH_2
10	CH_3CO-RIDVKDTKEALDKIEGC-NH_2
11	CH_3CO-LDKIEEEQNKSKKKAGC-NH_2
12	CH_3CO-SKKKAQQAAADTGNNGC-NH_2
13	CH_3CO-DTGNNSQVSQNYGC-NH_2

Figure 1. The construction of MA-based overlapping peptide library.

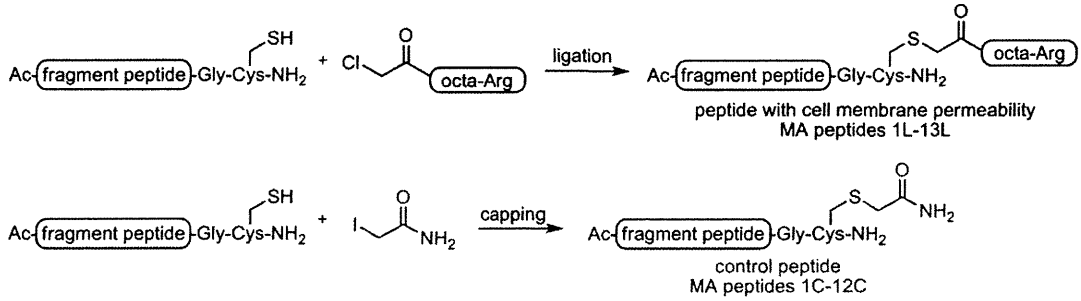

Figure 2. The design of MA peptides with cell membrane permeability (upper) and their control peptides (lower).

residues to preserve secondary structures (Fig. 1). Cys residues of the original MA sequence were changed into Ser residues because of the facility of peptide synthesis. Thirteen MA fragment peptides (1–13) were designed with the addition of Gly as a spacer and Cys as a conjugation site at the C-terminus. To impart cell membrane permeability to these peptides, the N-terminal chloroacetyl group of an octa-arginyl (R_8) peptide[19] was conjugated to the side-chain thiol group of the Cys residue of the above peptides. This resulted in the MA peptides 1L–13L (Fig. 2). R_8 is a cell membrane permeable motif and its fusion with parent peptides is known to produce bioactive peptides with no significant adverse properties.[12,13,20–24] In addition, the R_8-fusion can increase the solubility of MA

Table 1
Anti-HIV activity and cytotoxicity of control MA peptides

MA peptide	MT-4 cell	PM1/CCR5 cell		MT-4 cell
	NL4-3 (MTT assay) EC_{50}[a] (μM)	NL(AD8) (MTT assay) EC_{50}[a] (μM)	JR-CSF (p24 ELISA) EC_{50}[a] (μM)	(MTT assay) CC_{50}[b] (μM)
1C	>50	ND	ND	>50
2C	17 ± 1.4	1.0	ND	>50
3C	>50	ND	ND	>50
4C	No inhibition at 12.5 μM	ND	ND	14
5C	>50	ND	ND	>50
6C	37 ± 12	24% inhibition at 6.25 μM	25% inhibition at 50 μM	>50
7C	>50	ND	ND	>50
8C	>50	ND	ND	>50
9C	29 ± 1.4	13	8.1	>50
10C	No inhibition at 12.5 μM	ND	ND	17
11C	>50	ND	ND	>50
12C	>50	ND	ND	>50
14C	>50	ND	ND	>50
AZT	0.020	0.459	0.17	>100
SCH-D	ND	0.026	0.0014	ND

X4-HIV-1 (NL4-3 strain)-induced cytopathogenicity in MT-4 cells and R5-HIV-1 (NL(AD8) strain)-induced cytopathogenicity in PM1/CCR5 cells evaluated by the MTT assay, and inhibitory activity against R5-HIV-1 (JR-CSF strain)-induced cytopathogenicity in PM1/CCR5 cells evaluated by the p24 ELISA assay.

[a] EC_{50} values are the concentrations for 50% protection from HIV-1-induced cytopathogenicity in MT-4 cells.

[b] CC_{50} values are the concentrations for 50% reduction of the viability of MT-4 cells. All data are the mean values from at least three independent experiments. ND: not determined.

Table 2
Anti-HIV activity and cytotoxicity of MA peptides with cell membrane permeability

MA peptide	MT-4 cell	PM1/CCR5 cell		MT-4 cell
	NL4-3(MTT assay) EC_{50} (μM)	NL(AD8)(MTT assay) EC_{50} (μM)	JR-CSF(p24 ELISA) EC_{50} (μM)	(MTT assay) CC_{50} (μM)
1L	30	30	40	>50
2L	21 ± 4.2	>31	ND	32 ± 4.2
3L	no inhibition at 25 μM	ND	ND	36
4L	no inhibition at 3.13 μM	ND	ND	3.7
5L	40	42% inhibition at 50 μM	42	>50
6L	40 ± 8.9	49% inhibition at 50 μM	31	>50
7L	35 ± 1.5	37% inhibition at 50 μM	35% inhibition at 50 μM	>50
8L	2.3 ± 0.3	5.8	7.8	9.0 ± 2.4
9L	2.1 ± 0.5	0.43	0.58	5.7 ± 2.1
10L	43 ± 8.5	42% inhibitionat 50 μM	27	>50
11L	18 ± 3.0	17% inhibition at 25 μM	23	>50
12L	41 ± 5.5	30% inhibition at 25 μM	27	>50
13L	20 ± 2.1	0.43	11	>50
14L	no inhibition at 25 μM	ND	ND	36
AZT	0.020	0.459	0.17	>100
SCH-D	ND	0.026	0.0014	ND

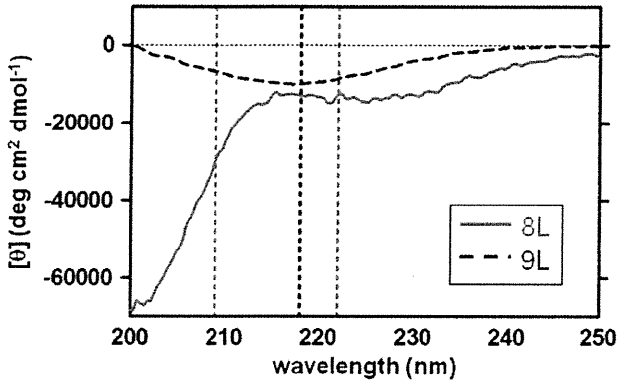

Figure 3. CD spectra of MA peptides 8L (28 μM) and 9L (65 μM) in PBS buffer, pH 7.4 at 25 °C.

peptides whose hydrophobicity is relatively limited. On the other hand, to develop control peptides lacking cell membrane permeability, iodoacetamide was conjugated to the thiol group of the Cys residue to prepare MA peptides 1C–12C (Fig. 2). MA peptide 13C was not synthesized because MA fragment 13 is insoluble in PBS buffer.

The anti-HIV activity of MA peptides 1L–13L and MA peptides 1C–12C, was evaluated. Inhibitory activity against T-cell line-tropic (X4-) HIV-1 (NL4-3 strain)-induced cytopathogenicity in MT-4 cells and against macrophage-tropic (R5-) HIV-1 (NL(AD8) strain)-induced cytopathogenicity in PM1/CCR5 cells was assessed by the 3-[4,5-dimethylthiazol-2-yl]-2,5-diphenyltetrazolium bromide (MTT) assay, and inhibitory activity against R5-HIV-1 (JR-CSF strain) replication in PM1/CCR5 cells was determined by the p24 ELISA assay. The results are shown in Tables 1 and 2. The control MA peptides 6C and 9C showed slight anti-HIV activity against NL4-3, NL(AD8) and JR-CSF strains, and 2C showed high anti-HIV activity against NL4-3 and NL(AD8) strains, but the other control MA peptides showed no significant anti-HIV activity. 2C showed significant anti-HIV activity against both X4-HIV-1 and R5-HIV-1 strains, suggesting that this region of the MA domain is relevant with Gag localization to the plasma membrane (PM)[25] and that 2C might inhibit competitively the interaction between MA and PM. On the other hand, the MA peptides with the exception of 3L and 4L, showed moderate to potent anti-HIV activity against all three strains. These peptides expressed almost the same level of anti-HIV activity against both X4-HIV-1 and R5-HIV-1 strains. The MA peptides 8L and 9L in particular, showed significant anti-HIV activity. These results suggest that MA peptides achieve entry into target cells as a result of the addition of R_8, and inhibit viral replication within the cells. The adjacent peptides 8L and 9L possess an overlapping sequence TIAVL. Such peptides exhibited relatively high cytotoxicity and the MA peptide 4L showed the highest cytotoxicity although it did not show any significant anti-HIV activity. The control MA peptides 1C–12C were relatively weakly cytotoxic. The MA peptides 8C and 9C exhibited no significant cytotoxicity, although the addition of R_8, giving 8L and 9L, caused a remarkable increase in cytotoxicity. This suggests that the octa-arginyl (R_8) sequence is correlated with the

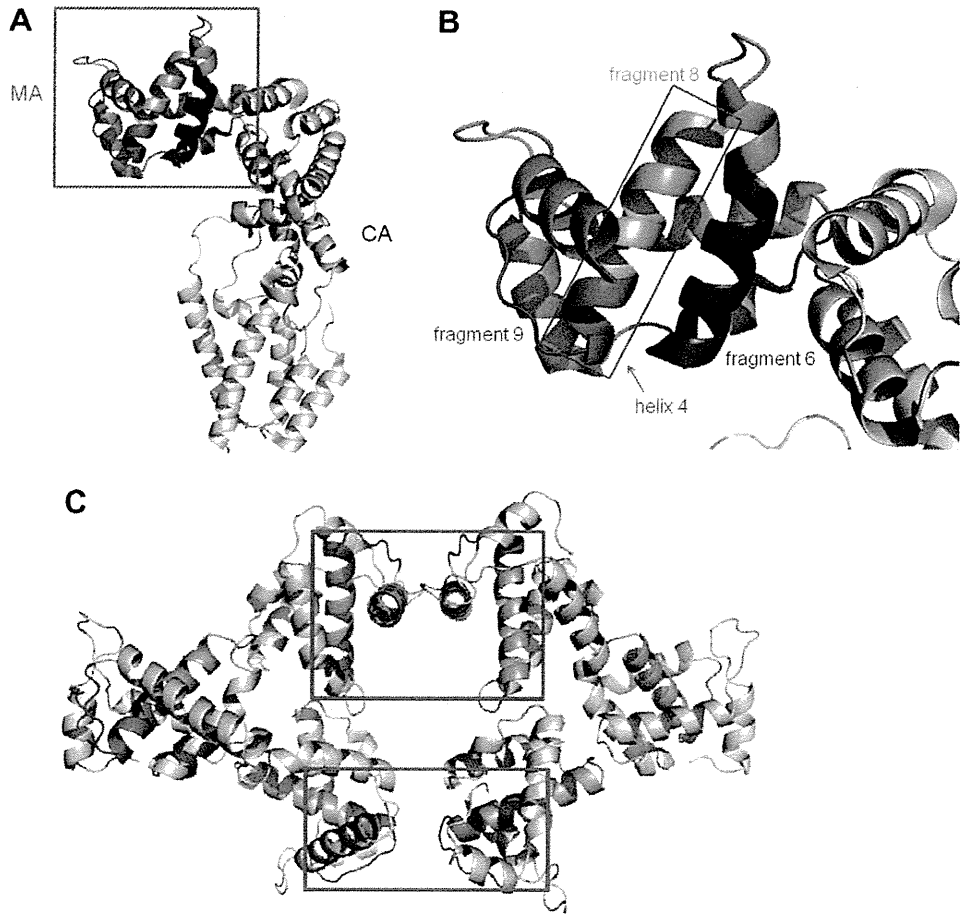

Figure 4. (A) The complete structure of MA and CA proteins (PDB ID: 2gol). (B) The enlarged structure of the highlighted region of (A). (C) The structure of an MA hexamer. Red-colored squares show interfaces between two MA trimers (PDB ID: 1hiw). Orange- and pink-colored helical ribbons represent fragments 8 and 9, respectively.